30

V.A. Lebedev

THE SUPER COLLIDER TRANSVERSE
FEEDBACK SYSTEM FOR SUPPRESSION
OF THE EMITTANCE GROWTH
AND BEAM INSTABILITIES
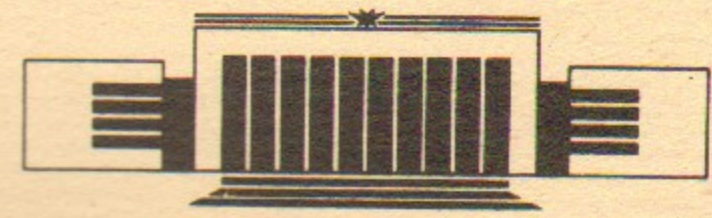
The Super Collider Transverse Feedback System for Suppression of the Emittance Growth and Beam Instabilities

Valery A. Lebedev

Budker Institute of Nuclear Physics,
630090 Novosibirsk-90, Russia

Abstract

A super collider transverse feedback system should suppress injection errors, emittance growth due to external noises, and beam instabilities. It is supposed that the feedback system should consist of two circuits: an injection damper operating just after injection and a super damper. To damp the emittance growth, the superdamper has to operate with the ultimate decrement close to the revolution frequency. The physics of such a feedback system and its main limitations are discussed in this article.

1. Introduction

The luminosity is one of the most important parameters among the main parameters of the Superconducting Super Collider. To reach the required luminosity, one needs high beam current, low beam emittance and durable beam lifetime what conditions very stringent requirements to the beam stability. In this case, the role of the feedback system for suppression of beam instabilities and emittance growth is very important.

The main purposes of the transverse feedback systems are the damping of the emittance increase due to injection errors, suppression of transverse multibunch instabilities and new task, unusual for previous colliders, i.e. the suppression of the emittance growth produced by external noise. Thus, the two main regimes of the feedback system operation can be distinguished.

The first one is the damping just after injection. The damping decrement at this stage should be high enough to suppress the emittance increase due to injection errors. The frequency band at this regime is determined by a time distance between batches (1.7 μs) and should be an order of ~0.5 MHz.

After initial damping, the long term damping system has to be switched on. Further we will call this system the superdamper. The system should operate all time of storage (except short time just after each next injection from HEB), acceleration and collisions of the beams. To prevent the emittance growth due to own noise, the system should have the noise of electronic referenced to the BPM resolution smaller than 1 μm. Because of this system operates on the already damped beam, its power can be much lower than for the injection damper.

This article is devoted to the analysis of the main requirements to the long term system and analysis of its operation. The theory of the feedback system with ultimate decrement and the theory of the emittance growth under feedback system noise are developed as well.

2. Coherent Instabilities

We will start our study from review of beam instabilities whose determine the initial requirements to the super damper.

2.1 Transverse Final Wall Resistivity Instability

Because of a very large circumference of the collider, the instability of the final wall resistivity is one of the most dangerous. For the collider with a two layer round vacuum chamber its increment can be expressed by the next formula[1]

$$\lambda_n = \frac{IecR}{Ev_0 a^3} \begin{cases} \dfrac{1}{\sqrt{2\pi\sigma_1\omega_n}}, & \delta_1 \ll d_1, \\[3mm] \dfrac{c}{2\pi(\sigma_1 d_1 + \sigma_2 d_2)\omega_n}, & \delta_{1,2} \gg d_{1,2}, \end{cases} \qquad (1)$$

where I is the beam current, R is the average storage ring radius, E is the beam energy, c is the light velocity, v_0 is the betatron tune, $\omega_n = |\omega_0(v_0-n)|$ is the frequency of the mode n, ω_0 is the revolution frequency, a is the vacuum chamber radius, σ_1, σ_2, d_1, d_2 are the conductivities and thicknesses of internal (copper) and external (stainless steel) layers,

$$\delta_{1,2} = \frac{c}{\sqrt{2\pi\sigma_{1,2}\omega_n}}, \qquad (2)$$

are skin layer thicknesses. We neglect from here a coupling between the vertical and horizontal motions so that v_0 denotes the tune related to the chosen direction (vertical or horizontal one). For the SSC the bottom and upper parts in Eq.(1) can be used for $f < 17$ kHz and $f > 17$ kHz, consequently. Note also that the bottom part of Eq.(1) is justified for sufficiently high frequencies

$$\omega > \omega_c \equiv \frac{c^2}{2\pi a}\left(\frac{1}{d_1\sigma_1} + \frac{1}{d_1\sigma_1}\right), \qquad (3)$$

so that magnetic field is still small outside the vacuum chamber (for the SSC vacuum chamber $\omega_c/2\pi \approx 90$ Hz). As can be seen from Eq.(1) the instability increment is proportional to $1/\omega$ at low frequencies and to $1/\omega^{1/2}$ at high frequencies. The results of calculations at injection ($E = 2$ TeV, $I = 70$ mA, $a = 17$ mm, $d_1 = 0.1$ mm, $\sigma_1^{-1} = 5.6 \cdot 10^{-8}$ Ω/cm (RRR=30), $d_2 = 3$ mm, $\sigma_2^{-1} = 8.5 \cdot 10^{-5}$ Ω/cm) are shown in Figure 1. We suppose here that the collider vacuum chamber in warm
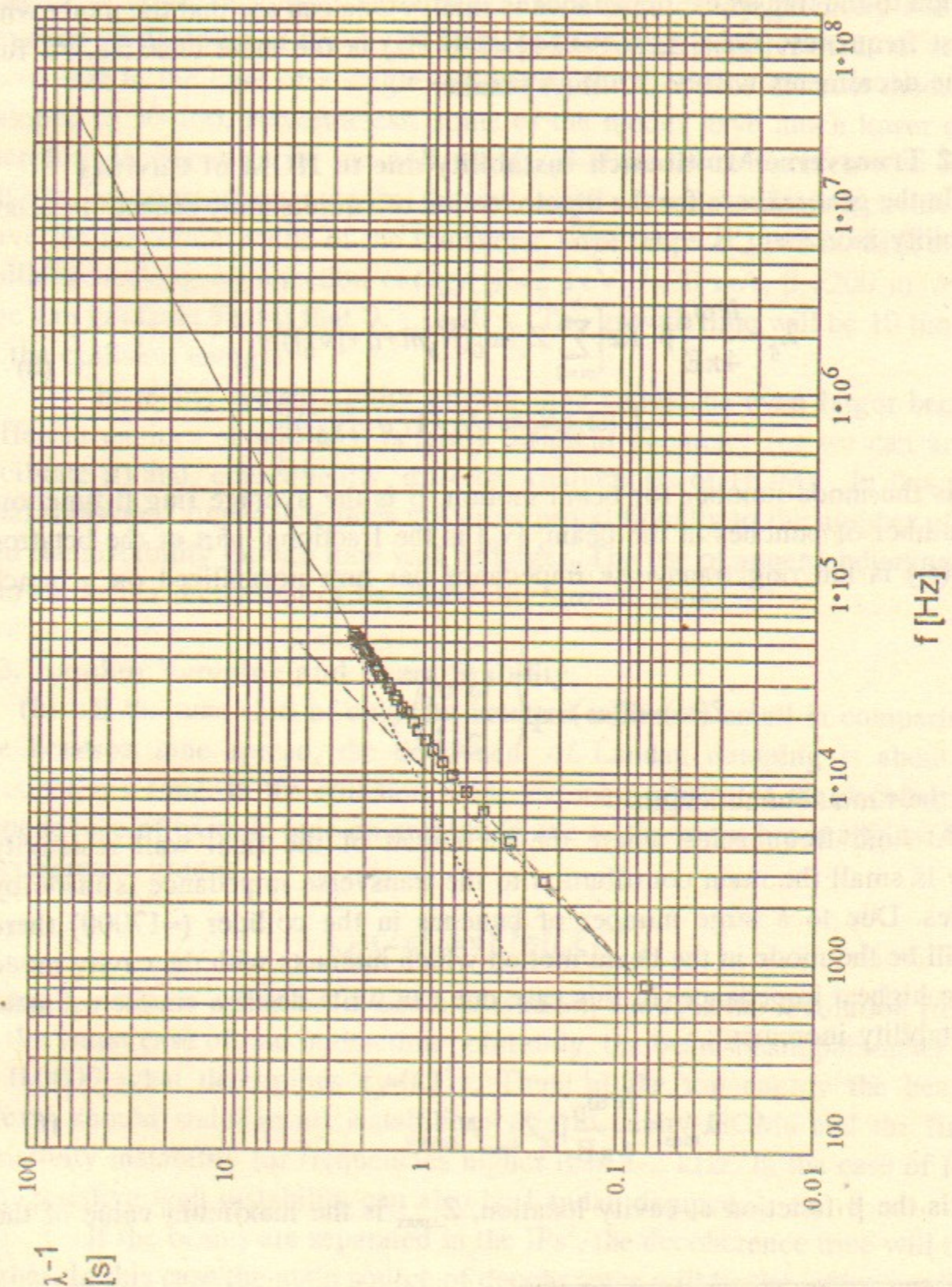
Figure 1. Dependance of growth time of the final wall resistivity instability on frequency.

straight sections is produced of a substance with high conductivity, and their contribution to the transverse impedance is small[1]. One can see that the mode with the lowest frequency ($f=f_0 \cdot |\,123.78-124\,|=760$ Hz) is the most unstable. At full energy the decrements will be 10 times smaller.

2.2 Transverse Multibunch Instability due to HOM of Cavities

In the general case for the dipole motion of equidistantly spaced bunches the instability increment is equal to[2]

$$\lambda_q = \frac{Ie\omega_0}{4\pi E}\beta \; Re\left[\sum_{m=0}^{\infty} Z_\perp(\omega_0(N_b m+q+[\nu_0]))- \\ -Z_\perp(\omega_0(N_b m+N_b+1-q-[\nu_0]))\right], \qquad (4)$$

where q is the mode number for beam motion, β is the average ring β-function, N_b is a number of bunches in the beam, $[\nu_0]$ is the fractional part of the betatron tune, $Z_\perp(\omega)$ is the ring transverse impedance per turn normalized on a bunch length

$$Z(\omega)\rightarrow Z(\omega)\exp\left(-\frac{\omega^2\sigma_s^2}{2c^2}\right), \qquad (5)$$

and σ_s is the r.m.s. bunch length.

At high frequencies where the increment of the final wall resistivity instability is small the main contribution to the transverse impedance is made by RF cavities. Due to a large number of bunches in the collider (≈ 17000) there always will be the mode in the beam motion which interacts with the cavity mode having the highest impedance. In this case one can write down a simple estimate of the instability increment:

$$\lambda_{max} \approx \frac{Ie\omega_0}{4\pi E}\beta_c Z_{\perp max} N_{cavity} \qquad (6)$$

where β_c is the β-function at cavity location, $Z_{\perp max}$ is the maximum value of the

---

[1]The total length of warm sections is about 10% of the orbit length, so that for the aluminum vacuum chamber with wall thickness of 3 mm the contribution of warm sections to the transverse impedance will be less than 10%.

transverse impedance of one cavity, and N_{cavity} is a number of cavities. The transverse impedance has a weak dependance from cavity geometry and strongly depends on damping of the cavity HOMs. The experiments carried out at SLAC[3] show that in the case of a single cell cavity the Q-values of most modes can be damped to 30-100. Nevertheless, some of the modes have much lower damping, therefore in our estimate we will use $Q_{max}\approx 1000$ that coincides with $Z_{\perp max}\approx 0.5$ MΩ/m. For comparison, note that the undamped normal conducting cavities usually have the maximum value of the transverse impedance $Z_{\perp max}\approx 5$-10 MΩ/m. For the collider working on injection energy (E=2 TeV, I=70 mA, β_c=200 m, N_{cavity}=32) one can get from Eq.(4) that $\lambda^{-1}_{max}\approx 10$ s. The growth time will be 10 times larger at the collision energy.

In reality the instability growth time should be even larger because the different cavities should have slightly different geometry (or we can artificially facilitate it) and, consequently, different frequencies of HOMs. In this case, the total transverse impedance does not grow proportionally to the number of cavities and the instability growth time will be larger. The use of superconducting cavities allows further increasing of the instability growth time.

2.3. Landau Damping and Beam Stability

If the tune shift of coherent betatron motion is small in comparison with the betatron tune spread, the decrement of Landau damping is about inverse decoherence time. In the collision mode the main source of the decoherence is a dependence of particle tune on amplitude due to the beam-beam effects. Then the decoherence time is

$$\tau_d \approx (2\pi f_0\Delta\nu)^{-1}\approx(f_0\xi)^{-1}, \qquad (7)$$

where ξ is the so-called beam-beam parameter, and f_0 is the revolution frequency. In the worst case of one interaction point only, the beam-beam parameter is equal to 0.0009 what determines $\tau_d\approx 0.3$ s. Thus, at the top energy the beam-beam effects should stabilize all instabilities due to cavity HOMs and the final wall resistivity instability for frequencies higher than 1-2 kHz. In the case of four IPs, the resistive wall instability can also be Landau damped.

If the beams are separated in the IPs[2], the decoherence time will be much higher. In this case the main source of decoherence will be the lattice nonlinearity.

---

[2]It always occurs at injection and during beam storage and acceleration.

As follows from computer simulations[4], the expected betatron tune spread should be an order of $\Delta\nu\approx5\cdot10^{-5}$ ($\tau_d\approx1$ s) at injection energy and $\Delta\nu\approx5\cdot10^{-6}$ ($\tau_d\approx10$ s) at the top energy. This value is comparable with the real part of the coherent tune shift due to the wide band ring impedance whose value is

$$\Delta\nu_{wb}\approx\frac{eI_bR}{4\pi E\nu_0}Z_{\perp}(c/\sigma_s) \ . \qquad (8)$$

Here $I_b=eNc/(2\pi)^{1/2}\sigma_s$ is the peak bunch current, σ_s is the r.m.s. bunch length and $Z_{\perp}(\omega)$ is the transverse ring impedance. It follows from Eq.(8) that $\Delta\nu_{wb}\approx5\cdot10^{-5}$ for $Z_{\perp}\approx4$ MΩ/m and E=2 TeV. One can see that this value is close to the expected particle tune spread. The considered value of the transverse impedance is rather optimistic[5]. If the transverse impedance has a higher value, the Landau damping should be suppressed by coherent tune shift and the instability of cavity HOMs should occur in the absence of the beam-beam effects at both the injection and top energies.

Note here that although the betatron tune spread due to lattice chromaticity can be larger than the ones considered above, its effect is suppressed by synchrotron motion and can be neglected in the decoherence process.

3. Transverse Emittance Growth and its Suppression by the Feedback System

Noise and ripples in the magnetic field of a storage ring produce the beam betatron motion which due to the betatron tune spread leads to the emittance growth and, consequently, to the luminosity reduction. It is especially dangerous for the Superconducting Super Collider because of a very small revolution frequency and beam emittance. The main sources of this external perturbation are the transverse displacements (oscillations) of quads and ripples and noise in dipoles and dipole correctors.

3.1. A Short Review of the Theory

As the measurements of ground motion at the SSC site (and also at other places in the world) show, the expected value of the quadrupole axis displacements due to natural and man produced ground motion is so large that the emittance should be doubled in 10-60 minutes after acceleration[6]. In the ref.[7] it was suggested to use the transverse feedback system for suppression of the emittance growth. Later the process of emittance growth due to noise and its suppression by

the transverse feedback system was carefully studied in refs.[8] and [9]. It was shown that in the general case, where the spectral density of external perturbation is a smooth function of frequency (i.e. the spectral density does not change significantly within the frequency band of betatron tune spread), the emittance growth rate could be approximated as

$$\frac{d\epsilon}{dt}\approx\xi^2\left(\frac{3.3}{g^2+3.3\xi^2}+67\right)\left(\frac{d\epsilon}{dt}\right)_0, \qquad \xi<0.1, \quad g\leq0.5 \ . \qquad (9)$$

Here $g=2\lambda/f_0$ is the dimensionless decrement of the feedback system, ξ is the beam-beam parameter,

$$\left(\frac{d\epsilon}{dt}\right)_0=\frac{\omega_0^2}{4\pi}\sum_{n=-\infty}^{\infty}\beta S(\omega_n), \qquad \omega_n=\omega_0(\nu_0-n). \qquad (10)$$

is the emittance growth rate without the feedback system, $S(\omega)$ is the spectral density of beam kicks summed over one turn and referenced to the β-function β. One can express this "summed" spectral density through the cross spectral density of angle kicks from different magnets

$$\beta S(\omega)=\sum_{i,j=1}^{N}\sqrt{\beta_i\beta_j}S_{ij}(\omega)\cos(\mu_i-\mu_j-\omega\tau_{ij}) \ . \qquad (11)$$

Here N is a number of magnets, β_i and β_j are the β-functions in magnets i and j, $\mu_i-\mu_j$ is the betatron phase advance between magnets i and j, τ_{ij} is the time of flight from magnet i to magnet j, S_{ij} is the cross spectral density of angle kicks for magnets i and j. This cross spectral density is bound up with the cross correlation function of angle kicks by the expression

$$K_{ij}(\tau_1-\tau_2)\equiv\langle\theta_i(\tau_1)\theta_j(\tau_2)\rangle=\int_{-\infty}^{\infty}S_{ij}(\omega)e^{i\omega(\tau_1-\tau_2)}d\omega \ , \qquad (12)$$

where $\theta_i(\tau)$ and $\theta_j(\tau)$ are the angles excited by kicks of magnets i and j. In the most of cases, one can consider that all the sources of noise are independent $S_{ij}=\delta_{ij}S_i$ so that Eq.(11) is simplified to

$$\beta S(\omega)=\sum_{i=1}^{N}\beta_iS_i(\omega) \ . \qquad (13)$$

Eqs.(9)-(13) are justified for both the vertical and horizontal planes. It is important to note that coupling between the vertical and horizontal motions should

redistribute the emittance growth between them so that for both transverse planes one can put: $d\epsilon/dt=((d\epsilon/dt)_x+(d\epsilon/dt)_y)/2$.

As follows from Eq.(10), the betatron resonance frequencies only contribute to the emittance growth. Usually the main contribution is determined by harmonic with the lowest frequency $\omega_\beta=\omega_0 min([\nu_0],1-[\nu_0])$ because the spectral density of perturbation drops very quickly with increasing frequency. Here $[\nu_0]$ is the fractional part of the betatron tune. For the Super Collider with the revolution frequency $\omega_0/2\pi=3441$ Hz and tune variation in the range $[\nu_0]\approx0.22-0.45$, this frequency is in the range 700-1500 Hz.

A survey of measurements of ground motion made in different locations and an estimate of the emittance growth in the collider on the basis of these measurements were performed in [6]. It was predicted that in the worst case the emittance growth time in the collider mode can have an order of 30 minute or even smaller. To have a required 24 hour beam life time, one needs the feedback suppression of the emittance growth at least 100.

3.2. General Requirements to the Feedback System

The general requirements to the feedback system are considered on an example of a simplified system with a sufficiently wide frequency band so that the motions of different bunches can be considered as independent. The feedback system consists of a beam position monitor (BPM), an amplifier and a kicker located a quarter betatron wave length downstream of the BPM. Let be for a transverse bunch displacement equal to x at the BPM location the bunch gets a kick in x-direction

$$\delta\theta=\frac{gx}{\sqrt{\beta_1\beta_2}} \qquad (14)$$

in the kicker. Here β_1 and β_2 are the β-functions at BPM and kicker locations. If the dimensionless gain g is much less than 1, the damping decrement of the system is

$$\lambda=\frac{g}{2}f_0 . \qquad (15)$$

It follows from Eq.(9) that for $g>\xi$ the suppression of the emittance growth by the feedback system is

$$S\equiv\frac{(d\epsilon/dt)_0}{(d\epsilon/dt)}\approx\frac{g^2}{(3.3+67g^2)\xi^2} . \qquad (16)$$

For four interaction points (IP) in the collider (ξ=0.0036) and an ultimate feedback system damping g=0.5-1, it gives $S\approx1000$. So we can conclude that to get the required emittance growth suppression the feedback system with ultimate damping should be used. The damping decrements in this case are much higher than for the damping of instabilities.

To prevent the emittance growth due to own noise, the feedback system has to have very small level of this internal noise. As follows from Eqs.(9) and (10) for the case where external noise is equal to zero, the emittance growth due to noise of the feedback system is equal to

$$\frac{d\epsilon}{dt}\approx\frac{\xi^2\omega_0^2}{4\pi}\left(\frac{3.3}{g^2+3.3\xi^2}+67\right)\sum_{n=-\infty}^{\infty}\frac{g^2}{\beta_1}S_{BPM}(\omega_n) . \qquad (17)$$

Here we take into account that in accordance with Eq.(14) the spectral density of the kick angle $S(\omega)$ is bound up with the spectral density of the feedback system noise $S_{BPM}(\omega)$ referenced to the BPM coordinate resolution

$$\beta S(\omega)=\beta_2\frac{g^2}{\beta_1\beta_2}S_{BPM}(\omega) . \qquad (18)$$

For a wide band noise we can express the sum in Eq.(17) through the BPM resolution

$$\omega_0\sum_{n=-\infty}^{\infty}S_{BPM}(\omega_n)\approx\int_{-\infty}^{\infty}S_{BPM}(\omega))d\omega=x_{BPM}^2 , \qquad (19)$$

thus, one has

$$\frac{d\epsilon}{dt}\approx\xi^2(3.3+67g^2)f_0\frac{x_{BPM}^2}{2\beta_1} . \qquad (20)$$

One can see from Eq.(20) that for $g\leq0.2$ the emittance growth rate practically does not depend on the gain value. For the emittance growth time of 24 hour we finally have that the BPM noise x_{BPM} has to be less than 1 μm.

4. The Theory of the Multi-Bunch System with Ultimate Gain

A necessity of very careful analysis of the feedback system operation is conditioned by the requirement to achieve the ultimate decrement of the feedback system.

The simplified scheme of the system is shown in Figure 2. Because of a very large circumference of the collider the BPM and the kicker are located in one straight section and a beam kick is applied at the next turn. In this case, the phase advance between the BPM and the kicker depends on a collider tune. To allow the collider operation on different tunes, a couple of BPMs shifted by $\pi/2$ in betatron phase is used. The mixture of their signals allows one to get the signal with required phase.

To get the ultimate BPM resolution the signals from the BPMs are used in the closed orbit correction system which should suppress the beam offset from the BPMs electrical center with an accuracy of about 5-10 μm. Because of the correction system has a time response of an order of 1 s it cannot suppress fast closed orbit variations in the BPM. To exclude them and to prevent from a saturation of the output amplifier it is suggested to use the notch filter. The idea of the filter is that the BPM signal from the previous turn is subtracted from the signal of the current turn. It removes the residual constant displacement of the closed orbit in the BPM and strongly suppresses its slow variations.

4.1. Bunch-by Bunch System with Notch Filter

First, we consider a wide band system where the motion of each bunch is independent of others.

Considering the particle motion in an accelerator, we will neglect the coupling between vertical and horizontal degrees of freedom and use the following variables:

$$X = \frac{x}{\sqrt{\beta}}, \qquad P = \beta \frac{d}{ds} \frac{x}{\sqrt{\beta}}, \qquad (21)$$

where s is the path length along orbit. The particle motion is suggested to be ideally linear so that the one turn mapping in the lattice is

$$\vec{V}_{n+1} = M \vec{V}_n, \quad \vec{V}_n = \begin{vmatrix} X_n \\ P_n \end{vmatrix}, \quad M = \begin{vmatrix} \cos(2\pi \nu_0) & \sin(2\pi \nu_0) \\ -\sin(2\pi \nu_0) & \cos(2\pi \nu_0) \end{vmatrix}, \qquad (22)$$

where X_n and P_n are the bunch coordinate and momentum, and n numerates a turn number. We also introduce the matrix of the coordinate transformation from the BPM to the kicker
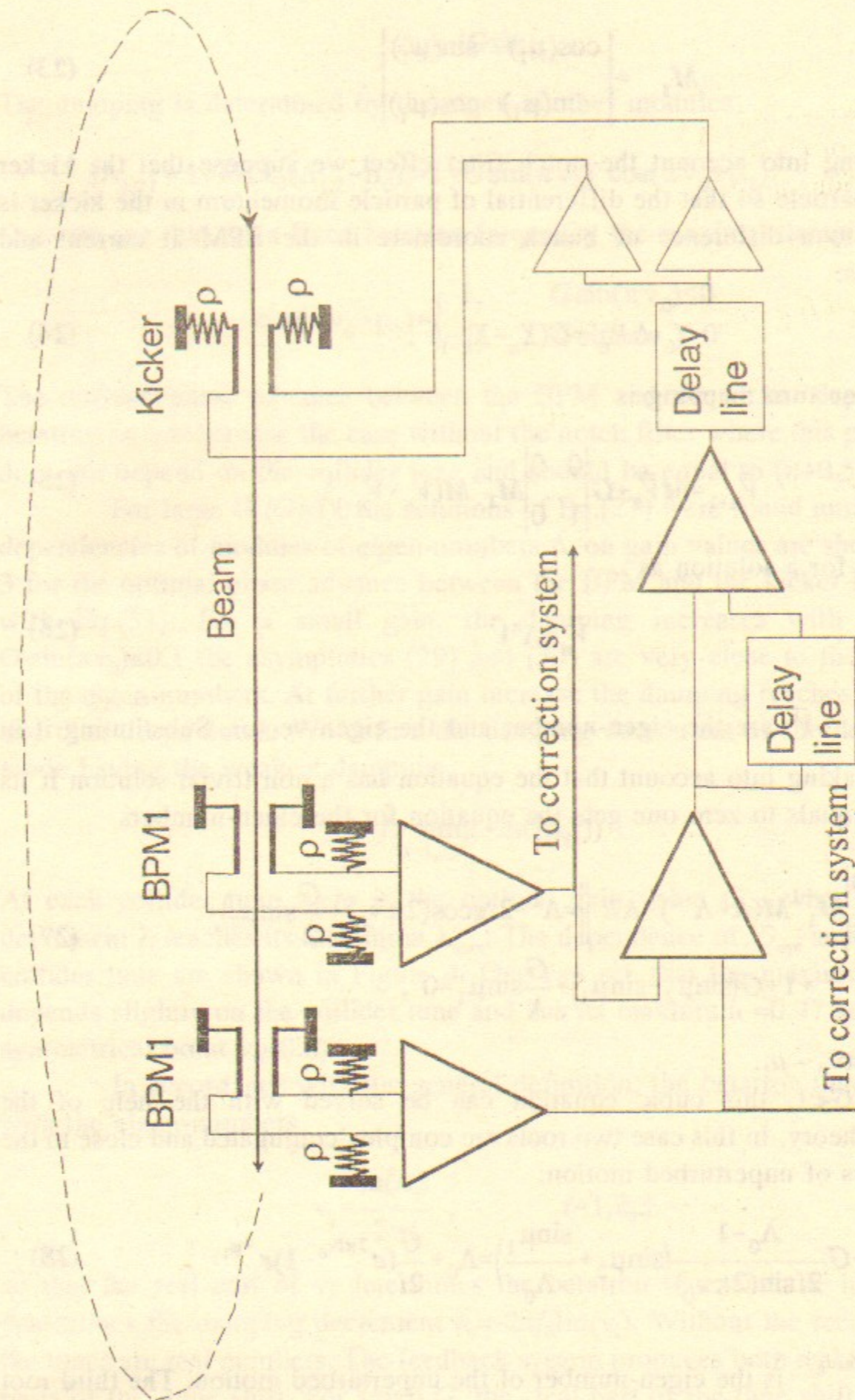
Figure 2. The symplified scheme of the feedback system, ρ=50 Ω.

$$M_1 = \begin{vmatrix} \cos(\mu_1) & \sin(\mu_1) \\ -\sin(\mu_1) & \cos(\mu_1) \end{vmatrix} . \qquad (23)$$

Taking into account the notch filter effect we suppose that the kicker deflects the particle so that the differential of particle momentum in the kicker is proportional to a difference of bunch coordinate in the BPM at current and previous turns:

$$\Delta P_n' = G(X_n - X_{n-1}) . \qquad (24)$$

Then a full one turn mapping is

$$\vec{V}_{n+1} = M\vec{V}_n + G \begin{vmatrix} 0 & 0 \\ 1 & 0 \end{vmatrix} M_1^{-1} M(\vec{V}_n - \vec{V}_{n-1}) . \qquad (25)$$

We will look for a solution as

$$\vec{V}_n = \Lambda^n \vec{V} , \qquad (26)$$

where Λ and $\vec{V}$ are the eigen-number and the eigen-vector. Substituting it in Eq.(25) and taking into account that the equation has a non trivial solution if its determinant equals to zero one gets the equation for the eigen-numbers

$$\left\| M + G \begin{vmatrix} 0 & 0 \\ 1 & 0 \end{vmatrix} M_1^{-1} M(\Lambda - \Lambda^{-1}) - \Lambda E \right\| = \Lambda^2 - 2\Lambda \left(\cos(2\pi\nu_0) + \frac{G}{2}\sin\mu_2 \right) +$$
$$+ 1 + G\left(\sin\mu_2 - \sin\mu_1\right) + \frac{G}{\Lambda}\sin\mu_1 = 0 , \qquad (27)$$

where $\mu_2 = 2\pi\nu_0 - \mu_1$.

For $G \ll 1$, this cubic equation can be solved with the help of the perturbation theory. In this case two roots are complex conjugated and close to the eigen-numbers of unperturbed motion:

$$\Lambda_1 = \Lambda_2^* \approx \Lambda_0 + G\frac{\Lambda_0 - 1}{2i\sin(2\pi\nu_0)}\left(\sin\mu_2 + \frac{\sin\mu_1}{\Lambda_0}\right) = \Lambda_0 + \frac{G}{2i}(e^{2\pi i\nu_0} - 1)e^{-\mu_1} . \qquad (28)$$

Here $\Lambda_0 = e^{2\pi i\nu_0}$ is the eigen-number of the unperturbed motion. The third root is close to zero (very high damping):

$$\Lambda_3 = -G\sin\mu_1 . \qquad (29)$$

The damping is determined by the eigen-number modules

$$|\Lambda_{1,2}| \approx 1 + Re(\Lambda_0^*(\Lambda_{1,2} - \Lambda_0)) = 1 + G\sin(\pi\nu_0)\cos(\pi\nu_0 + \mu_1). \qquad (30)$$

One can see that for a fixed betatron frequency the maximal damping is for

$$\cos(\pi\nu_0 + \mu_1) = \begin{cases} 1, & G\sin(\pi\nu_0) < 0 \\ -1, & G\sin(\pi\nu_0) > 0 \end{cases} . \qquad (31)$$

The optimal phase advance between the BPM and the kicker depends on the betatron tune otherwise the case without the notch filter where this phase advance does not depend on the collider tune and should be equal to $(n+0.5)\pi$.

For large G ($G \approx 1$), the solutions of Eq.(27) were found numerically. The dependencies of modules of eigen-numbers Λ_i on gain values are shown in Figure 3 for the optimal phase advance between the BPM and the kicker in accordance with Eq.(31). For a small gain, the damping increases with gain and at $G \cdot \sin(\pi\nu_0) \leq 0.1$ the asymptotics (29) and (30) are very close to the exact values of the eigen-numbers. At further gain increase the damping reaches its maximum and then drops down. We define the damping decrement as the decrement of a mode having the weakest damping

$$\lambda = f_0 \cdot \min_{i=1,2,3}(-\ln(|\Lambda_i|)) . \qquad (32)$$

At each collider tune there is the optimal gain value G_{opt} when the damping decrement λ reaches its maximum λ_{max}. The dependence of G_{opt} and λ_{max}/f_0 on the collider tune are shown in Figure 4. One can see that the maximum decrement depends slightly on the collider tune and has its maximum ≈ 0.47 at $\nu_0 \approx 0.4$ (or at symmetrical point $\nu_0 \approx 0.6$).

In accordance with the general definition, the betatron tune is bound up with the eigen-numbers

$$\nu_i = \frac{\ln(\Lambda_i)}{2\pi i} , \qquad i = 1, 2, 3. \qquad (33)$$

so that the real part of ν_i determines the betatron tune and the imaginary part determines the damping decrement $\lambda_i = -2\pi f_0 \text{Im}(\nu_i)$. Without the feedback system, the tunes are real numbers. The feedback system produces both real and imaginary parts of the tune shift. For small G, the real part of the tune shift is negligible, however, with an increase in G the real and imaginary parts of the tune are

ν=0.05

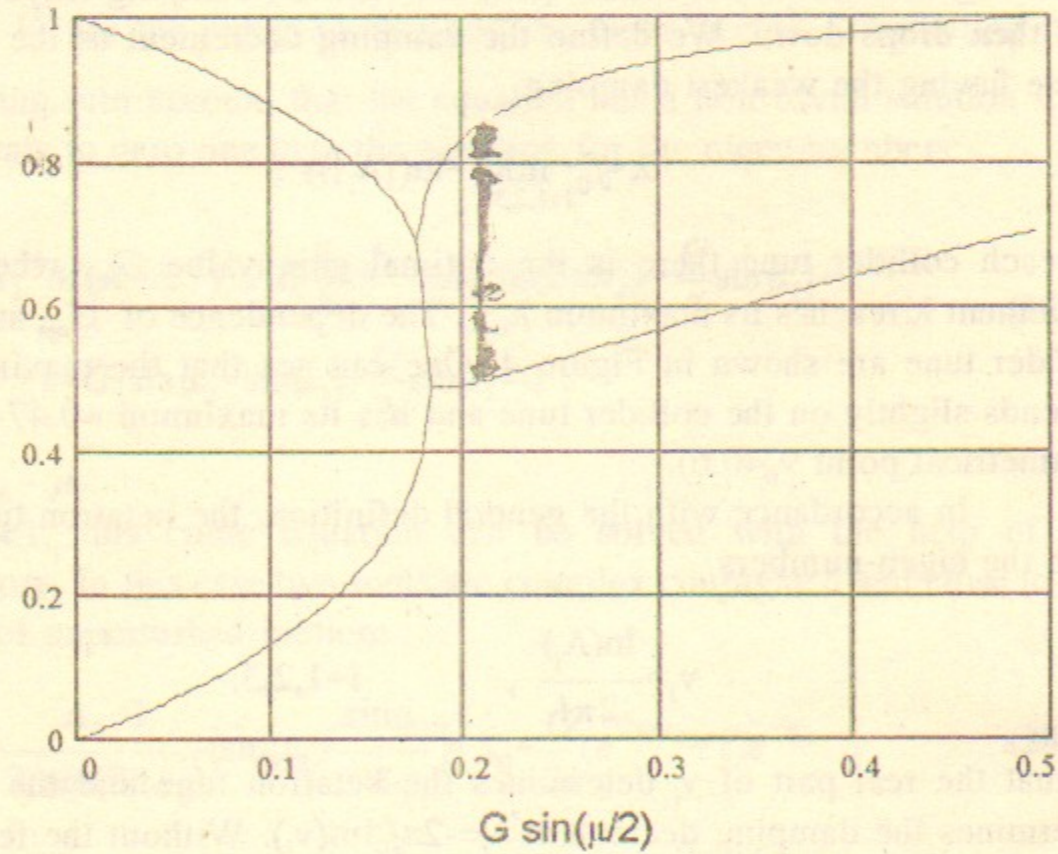$|\Lambda_{1,2,3}|$

G sin(μ/2)

ν=0.45

G sin(μ/2)
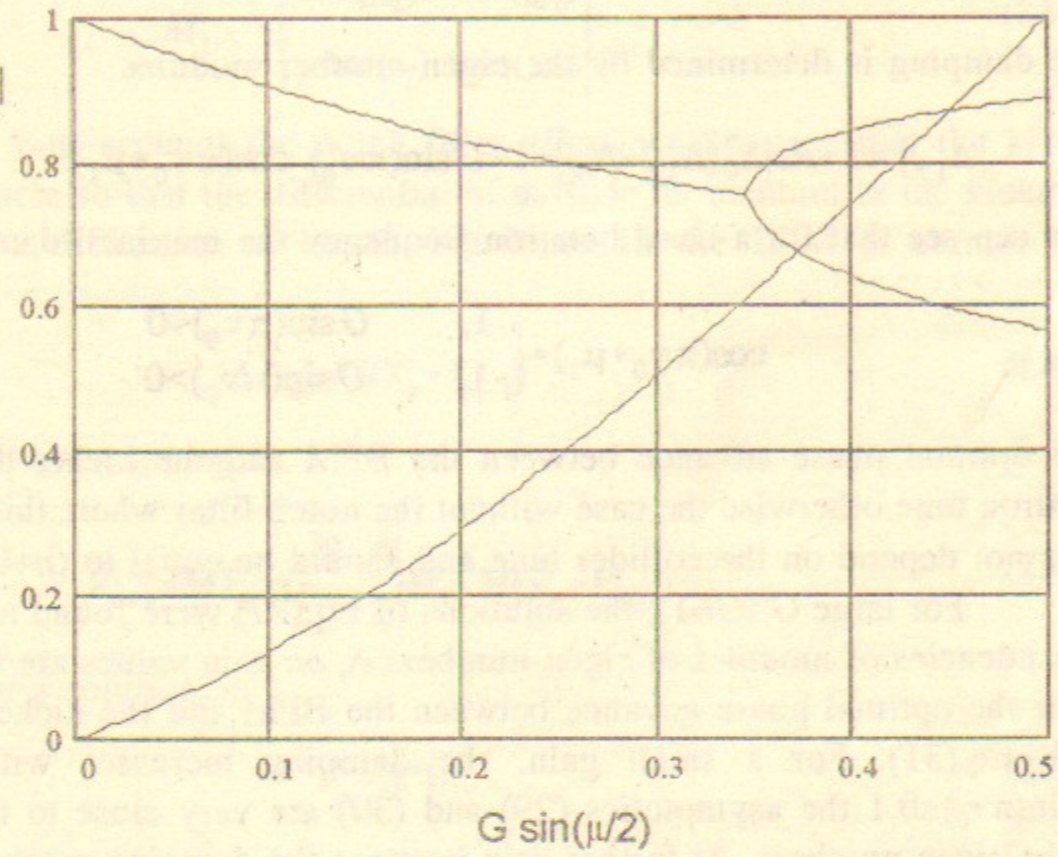
Figure 3. Dependance of modules of eigen-numbers on the feedback system gain, for betatron frequencies : $\nu_0=0.05$ and $\nu_0=0.45$.
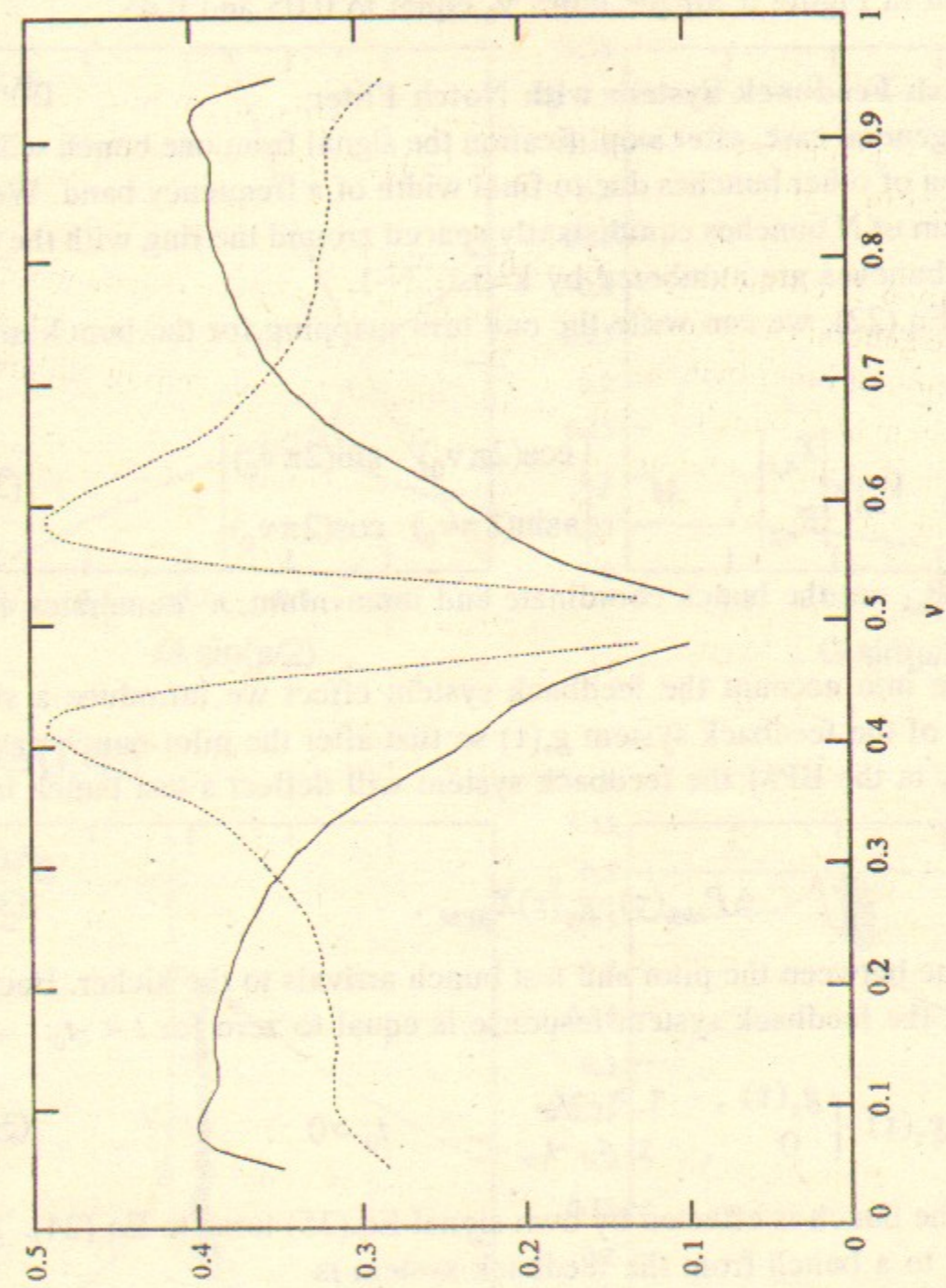

Figure 4. Dependencies of $G_{opt}\sin(\pi\nu)$ (solid line) and λ_{max}/f_0 (dotted line) on collider tune.

comparable. The dependence of real and imaginary parts of the tune on the gain value are shown in Figure 5 for the tunes v_0 equal to 0.05 and 0.45.

4.2. Multibunch Feedback System with Notch Filter

In the general case, after amplification the signal from one bunch will also affect the motion of other bunches due to final width of a frequency band. We will consider a system of N bunches equidistantly spaced around the ring with the same intensity. The bunches are numbered by k=0,1...N-1.

As in Eq.(22), we can write the one turn mapping for the bunch motion in the lattice

$$\vec{V}_{n+1,k}=M\vec{V}_{n,k} , \quad \vec{V}_{n,k}=\begin{vmatrix} X_{n,k} \\ P_{n,k} \end{vmatrix}, \quad M =\begin{vmatrix} \cos(2\pi v_0) & \sin(2\pi v_0) \\ -\sin(2\pi v_0) & \cos(2\pi v_0) \end{vmatrix}, \quad (34)$$

where $X_{n,k}$ and $P_{n,k}$ are the bunch coordinate and momentum, n numerates a turn number.

To take into account the feedback system effect we introduce a single bunch response of the feedback system $g_\tau(\tau)$ so that after the pilot bunch passage with offset X_{BPM} in the BPM the feedback system will deflect a test bunch in the kicker:

$$\Delta P_{kick}(\tau)=g_\tau(\tau)X_{BPM} . \quad (35)$$

Here τ is the time between the pilot and test bunch arrivals to the kicker. Because of the causality, the feedback system response is equal to zero for $t < -t_0$:

$$g_\tau(\tau)=\begin{cases} g_\tau(\tau) , & \tau > -t_0, \\ 0 , & \tau < -t_0, \end{cases} \quad t_0 >0 . \quad (36)$$
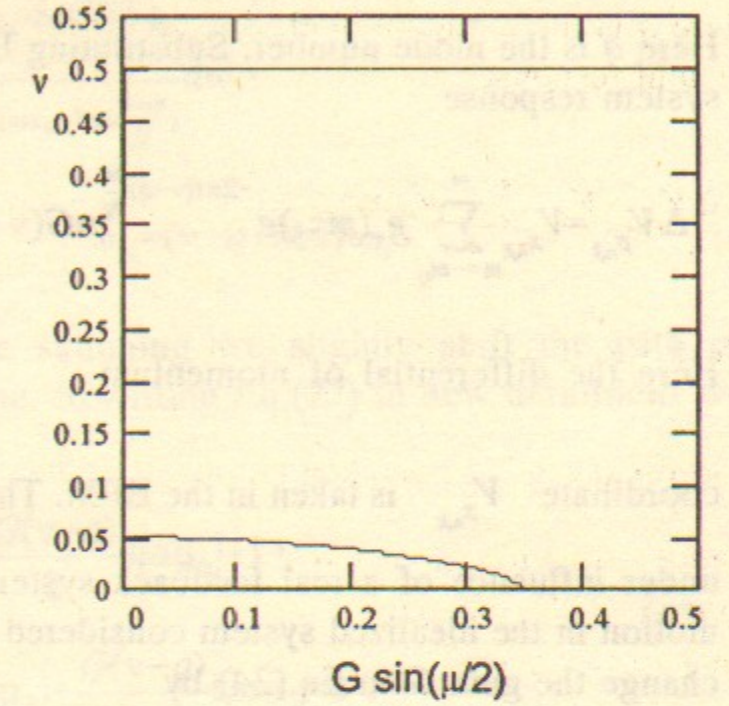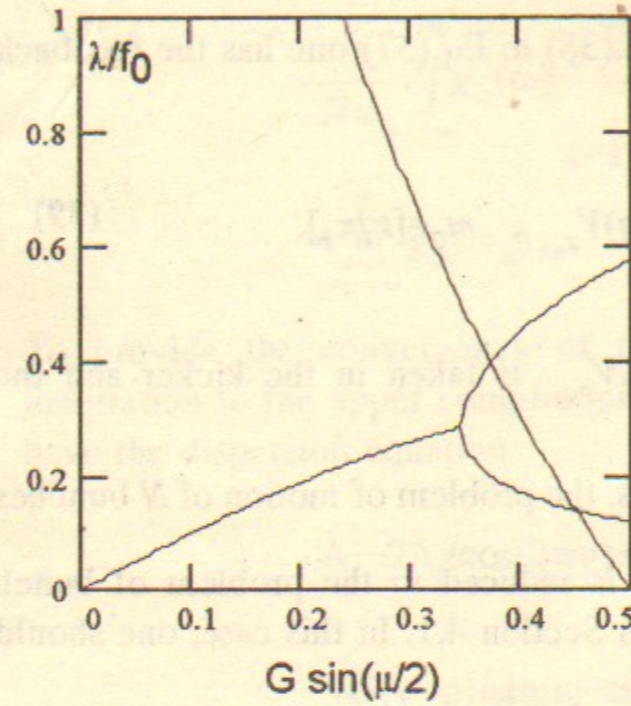
For $\tau=0$ when the bunch is effected by own signal Eq.(35) turns to Eq.(24). Then the kick applied to a bunch from the feedback system is

$$\Delta P_{n,k}=\sum_{m=0}^{\infty} g_\tau(m\tau_b)X_m . \quad (37)$$

Here m numerates all previous passages of bunches through the BPM, X_m are coordinates of bunches in the BPM, $\tau_b=T/N$ and T is the revolution time.
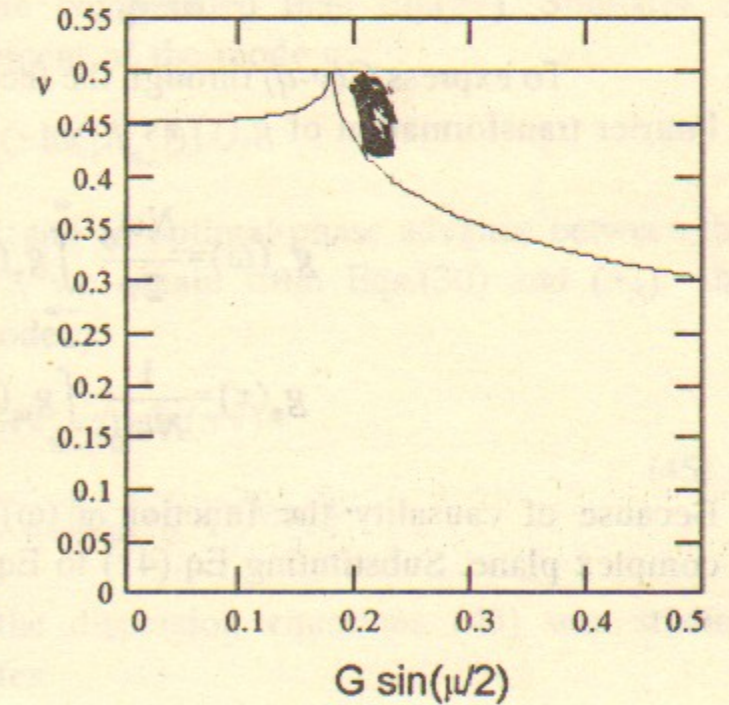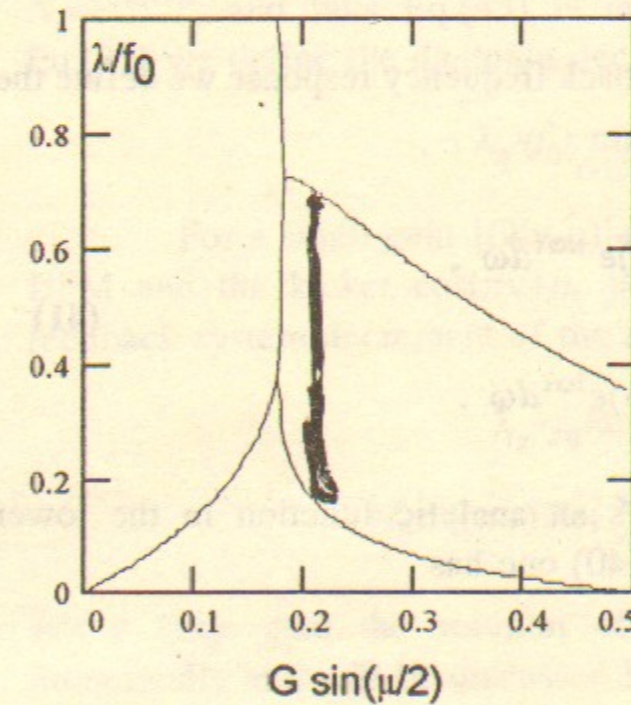
We will look for the solution as

$v=0.05$

$v=0.45$

Figure 5. Dependencies of decrements and coherent tune shifts on the feedback system gain.

$$\vec{V}_{n,k}=\vec{V}e^{2\pi i\nu n}e^{2\pi i(\nu-q)\frac{k}{N}}\equiv\vec{V}e^{2\pi i(\nu-q)\frac{m}{N}}, \quad \vec{V}_{n,k}=\left|\begin{matrix}V_x\\V_p\end{matrix}\right|_{n,k}, \quad m=Nn+k. \qquad (38)$$

Here q is the mode number. Substituting Eq.(38) to Eq.(37) one has the feedback system response

$$\Delta V_{p_{n,k}}=V_{x_{n,k}}\sum_{m=-m_0}^{\infty}g_\tau(m\tau_b)e^{-2\pi i(\nu-q)\frac{m}{N}}\equiv G(\nu-q)V_{x_{n,k}}, \quad m_0=[t_0/\tau_b]. \qquad (39)$$

Here the differential of momentum $\Delta V_{p_{n,k}}$ is taken in the kicker and the coordinate $V_{x_{n,k}}$ is taken in the BPM. Thus, the problem of motion of N bunches under influence of a real feedback system is reduced to the problem of bunch motion in the idealized system considered in Section 4.1. In this case, one should change the gain G in Eq.(24) by

$$G(\nu-q)=\sum_{m=-m_0}^{\infty}g_\tau(m\tau_b)e^{-2\pi i(\nu-q)\frac{m}{N}}. \qquad (40)$$

To express $G(\nu-q)$ through the feedback frequency response we define the Fourier transformation of $g_\tau(\tau)$ as

$$g_\omega(\omega)=\frac{N\omega_0}{2\pi}\int_{-\infty}^{\infty}g_\tau(\tau)e^{-i\omega\tau}d\omega ,$$

$$g_\tau(\tau)=\frac{1}{N\omega_0}\int_{-\infty}^{\infty}g_\omega(\omega)e^{i\omega\tau}d\omega . \qquad (41)$$

Because of causality the function $g_\omega(\omega)$ is an analytic function in the lower complex plane. Substituting Eq.(41) to Eq.(40) one has

$$G(\nu-q)=\frac{1}{N\omega_0}\sum_{m=-m_0}^{\infty}e^{-2\pi i(\nu-q)\frac{m}{N}}\int_{-\infty}^{\infty}g_\omega(\omega)e^{i\omega\tau_b m}d\omega=$$

$$=\frac{1}{N\omega_0}\int_{-\infty}^{\infty}g_\omega(\omega)\frac{e^{-i(\omega\tau_b-2\pi i\frac{\nu-q}{N})m_0}}{1-e^{-i(\omega\tau_b-2\pi i\frac{\nu-q}{N})}}d\omega= \qquad (42)$$

$$=\sum_{m=-\infty}^{\infty}g_\omega(\omega_m) , \qquad \omega_m=(\nu-q+Nm)\omega_0 .$$

To provide the convergency of the summing we slightly shift the path of integration to the upper complex plane. Rewriting Eq.(27) in new definitions we have the dispersion equation

$$\Lambda_q^2-2\Lambda_q\left(\cos(2\pi\nu)+\frac{G(\nu-q)}{2}\sin\mu_2\right)+1+$$

$$+G(\nu-q)\left(\sin\mu_2-\sin\mu_1\right)+\frac{G(\nu-q)}{\Lambda_q}\sin\mu_1=0 . \qquad (43)$$

Note that now the gain value $G(\nu-q)$ is the function of the eigen-number $\Lambda_q=e^{2\pi i(\nu-q)}$, and thus Eq.(43) is more complicated than Eq.(27). Similarly to Eq.(32) we define the damping decrement of the mode q:

$$\lambda_q=f_0\cdot\min_{i=1,2,3}(-\ln(|\Lambda_{q,i}|)) . \qquad (44)$$

For a small gain $|G(\nu-q)|\ll1$ and an optimal phase advance between the BPM and the kicker $\cos(\pi\nu+\mu_1)=-1$, we obtain from Eqs.(30) and (32) the feedback system decrement of the mode q

$$\lambda_q=f_0 Re\left(G(\nu_0-q)\right)\sin(\pi\nu)\equiv$$

$$\equiv f_0\sin(\pi\nu)Re\left(\sum_{m=-\infty}^{\infty}g_\omega(\omega_0(\nu_0-q+Nm))\right) . \qquad (45)$$

For a large gain the solution of the dispersion equations (43) was studied numerically and will be discussed later.

5. The Collider Transverse Feedback System.

As follows from previous sections the collider feedback system should

have the maximally possible damping at low frequencies (0.5-20) kHz, very small own noise, and also it seems very useful to have at least a small damping $(\lambda/f_0 \approx 10^{-4}-10^{-5})$ in high frequencies to suppress possible multibunch instabilities. Although the frequency band of the system can, in principle, be narrow, in reality the frequency response should be formed in a wide frequency band (up to 30 MHz) to prevent instabilities due to the feedback system itself.

Figure 6. The BPM cross section.
1- vacuum chamber,
2 - BPM electrodes.

The first question to be solved is the choice of a frequency range. Although the use of low frequencies seems very attractive, it has some serious difficulties. The first one is a very complicated problem of suppression of power line harmonics (n·60 Hz). And the second one is a requirement to provide the beam stability for all 16000 modes. As follows from Eq.(45), to get the beam stability, a phase shift of the feedback system gain for all modes should be smaller than $\pi/2$, that is, an amplification should not fall down faster than $1/\omega$. Thus, a necessity of very high amplification at low frequencies begets a sufficiently high amplification in the whole frequency range of 30 MHz, i.e., the instability due to the feedback system can not be Landau damped. Thus, to reach a beam stability, one needs careful forming of the frequency response in a wide frequency band (0.5 kHz - 30 MHz). Taking into account a high power that is not a trivial task.

To avoid these difficulties, it is suggested to use a high frequency system. Because of frequency transfer (as can be seen from Eq.(45)) the frequency band can be shifted by the bunch frequency Nf_0=60 MHz. In this case the frequency band width of 30 MHz will be shifted to high frequencies (45-75 MHz) where we can easily form the required frequency response.

5.1. Frequency Response of the Feedback System

To determine the frequency response of the feedback system we consider an unbunched beam circulating in the ring with current I_0 and a harmonic displacement from the closed orbit at the BPM location
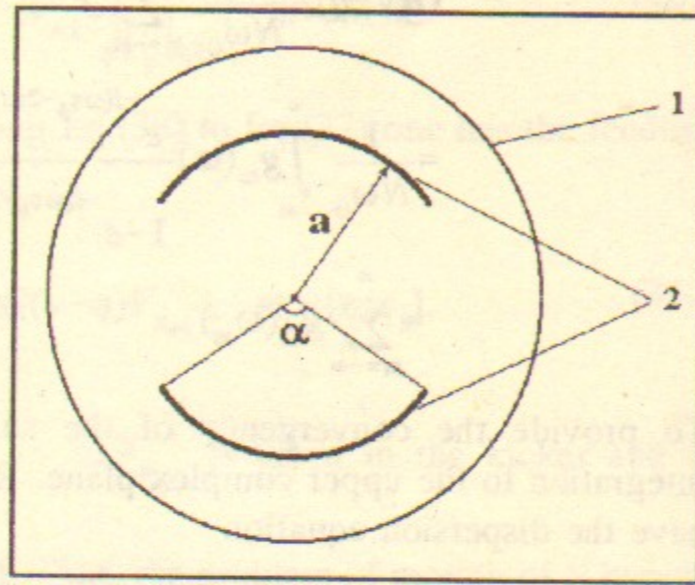
$$x(t) = x_0 e^{i\omega t} \quad . \tag{46}$$

Then, as follows from Eqs.(21) and (35), the beam deflection will be equal to

$$\frac{\Delta p_\perp}{p} = \frac{1}{\sqrt{\beta_1\beta_2}} \int_0^\infty x_0 e^{-i\omega t} g_\tau(t) \frac{I_0 dt}{eN_p} = g_\omega \frac{x_0}{\sqrt{\beta_1\beta_2}} \quad , \tag{47}$$

(compare with Eq.(14)). Here N_p is a number of particles in one bunch, and we use Eq.(41) to express $g_\tau(t)$ through g_ω.

From the other hand, for the strip line BPM and ultrarelativistic particles the differential voltage induced by the beam on BPM plates is

$$U_{BPM} = 2i \sin(\omega L/c) I_0 \frac{x_0}{a} Z_{BPM} \tag{48}$$

where L and a are the BPM length and radius of aperture and Z_{BPM} is the BPM coupling impedance. Its value is determined by the BPM wave impedance ρ (usually 50 Ω) and the angle width of BPM plates α visible from the BPM center (see Figure 6):

$$Z_{BPM} \approx \frac{2\sin(\alpha/2)}{\pi} \rho \quad . \tag{49}$$

The coupling impedance Z_{BPM} reaches its maximum value of $2\rho/\pi$ when each plate takes up a half of the full angle. We will use $\alpha = 50°$ and $\rho=12$ Ω in below estimates.

The kicker deflects the beam by the angle

$$\frac{\Delta p_\perp}{p} = \frac{2eU_0 L}{cpa} \frac{\sin(\omega L/c)}{\omega L/c}, \tag{50}$$

where $\pm U_0$ is a voltage amplitude on each of BPM plates, L and a are the kicker plate length and the radius of aperture. We suggest here that the BPM and the kicker have equal apertures and lengths.

Taking into account the total amplification of the system $K(\omega)$, we obtain the beam kick

$$\frac{\Delta p_\perp}{p} = i \frac{4eL Z_{BPM} I_0 K(\omega)}{cpa^2} \frac{\sin^2(\omega L/c)}{\omega L/c} x_0 \quad , \tag{51}$$

Comparing this equation with Eq.(47), we finally have the frequency response of

the feedback system

$$g_\omega(\omega)=i\frac{4eLZ_{BPM}I_0K(\omega)}{cpa^2}\frac{\sin^2(\omega L/c)}{\omega L/c}\sqrt{\beta_1\beta_2}\ ,\qquad(52)$$

5.2. Analyses of Feedback System Stability

For the analyses of the feedback system stability and damping we compiled the feedback system response from responses of BPM, amplifier, delay line and kicker:

$$g_\omega(\omega)=g_{BPM}(\omega)g_a(\omega)g_{delay}(\omega)g_{kick}(\omega)\quad .\qquad(53)$$

We modeled the BPM and the kicker as ideal strip lines whose frequency responses are

$$g_{BPM}(\omega)=i\cdot\sin(\omega L_{BPM}/c)\qquad(54)$$

for the BPM and

$$g_{kick}(\omega)=\frac{\sin(\omega L_{kick}/c)}{\omega L_{kick}/c}\qquad(55)$$

for the kicker, where L_{BPM} and L_{kick} are the BPM and kicker lengths. We choose these lengths of 125 cm to maximize the frequency responses on the central frequency of 60 MHz.

Because the general delay was taken into account in the equations of motion, we consider here only the deviation of delay time from the one turn delay so that

$$g_{delay}(\omega)=e^{-i\omega\tau_{delay}}\ .\qquad(56)$$

The frequency response of amplifier was modeled as

$$g_a(\omega)=g_0\frac{i\omega}{\omega_1+i\omega}\frac{\omega_2}{\omega_2+i\omega}\frac{1}{1+iQ_c\left(\frac{i\omega}{\omega_c}+\frac{i\omega_c}{\omega}\right)}\qquad(57)$$
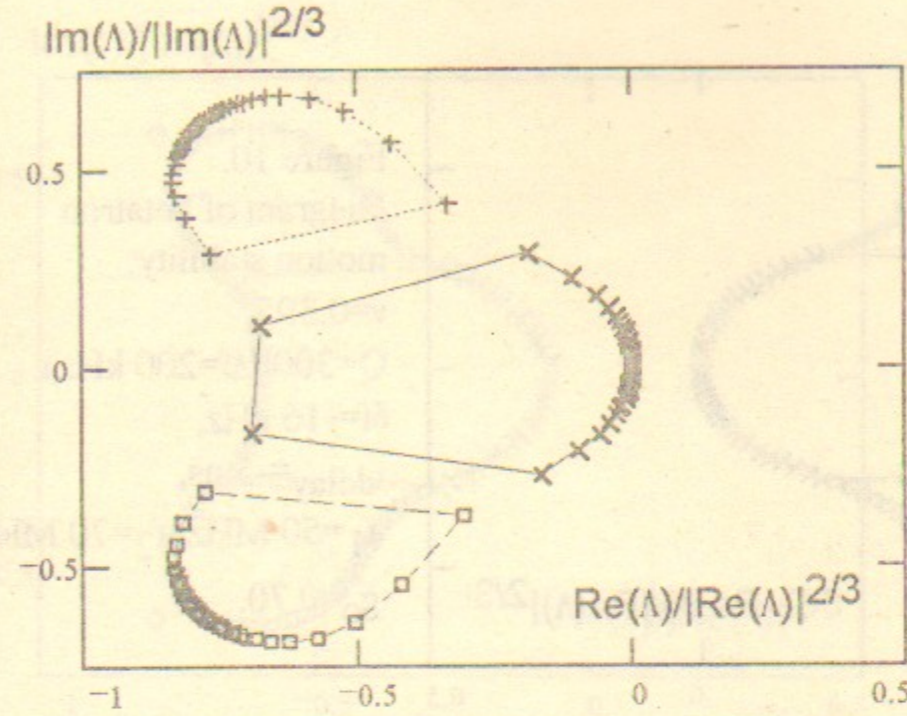
for a narrow band system and as

Figure 7.
Diagram of betatron motion stability;
$v=0.395$,
$Q=3000\ (\Delta f=20\ kHz)$,
$\delta f=-1.5\ kHz$,
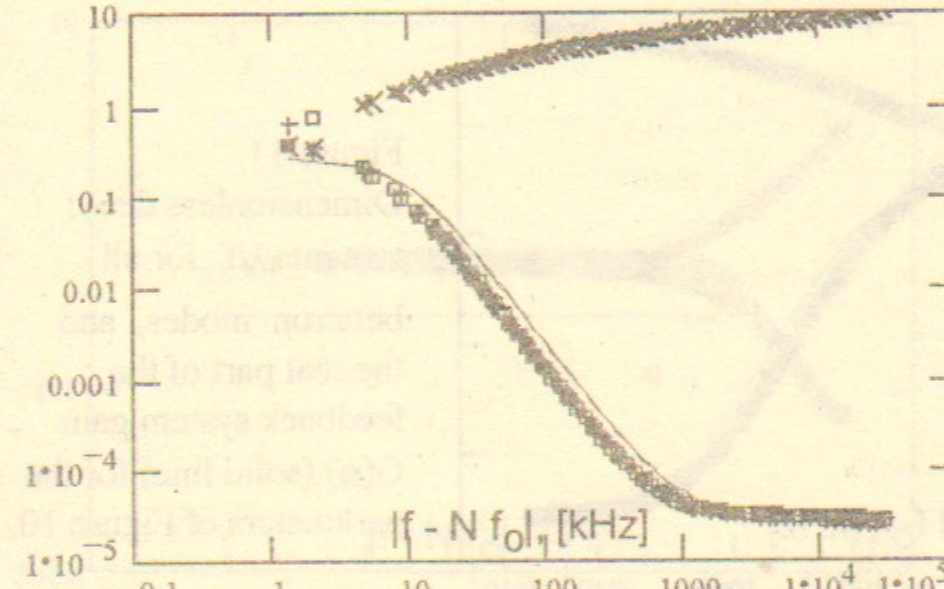$\tau_{delay}=-5\ ns$,
$f_1=50\ MHz,\ f_2=70\ MHz$,
$g_0=0.76$.

Figure 8.
Dimensionless decrements λ/f_0 for all betatron modes, and the real part of the feedback system gain $G(\omega)$ (solid line) for the parameters of Figure 7.
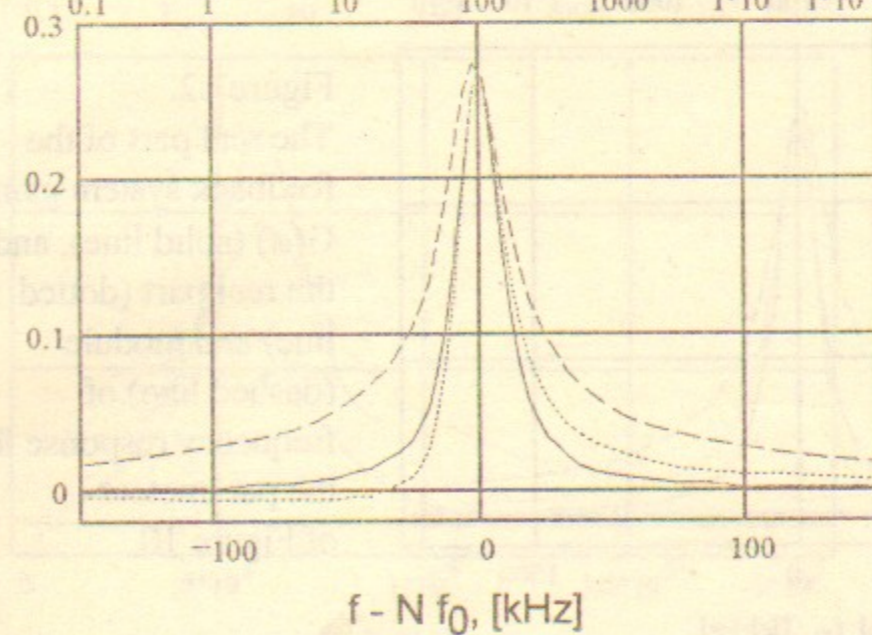
Figure 9.
The real part of the feedback system gain $G(\omega)$ (solid line), and the real part (dotted line) and module (dashed line) of frequency response for the parameters of Figure 7.
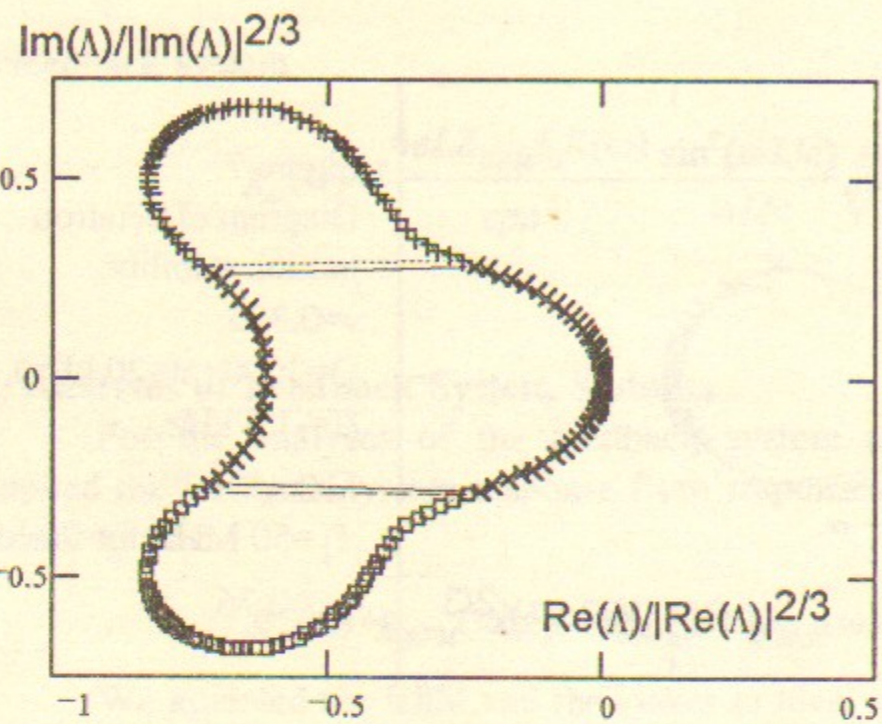
Figure 10.
Diagram of betatron motion stability;
$v=0.395$,
$Q=300$ ($\Delta f=200$ kHz),
$\delta f=-16$ kHz,
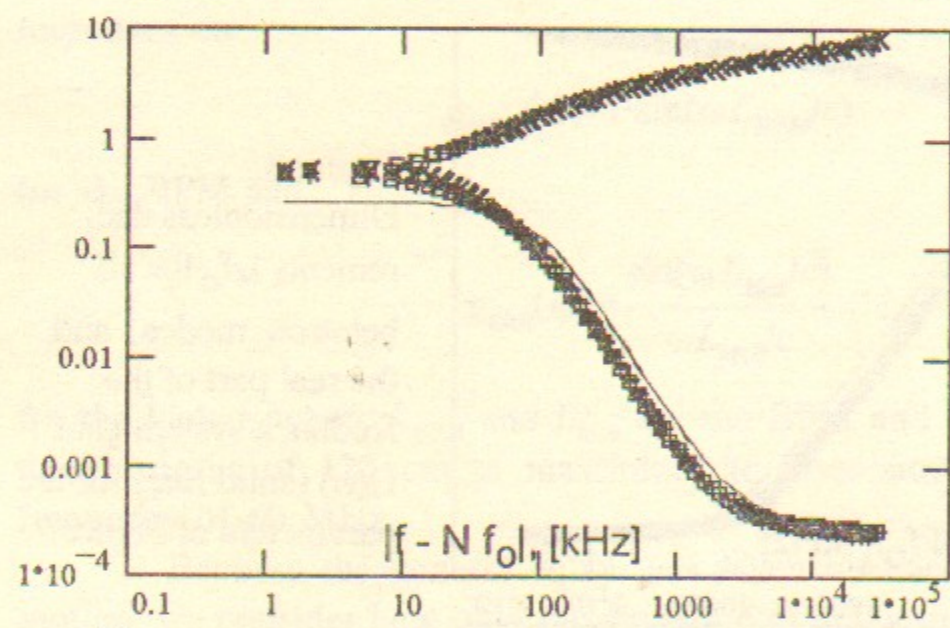$\tau_{delay}=-5$ ns,
$f_1=50$ MHz, $f_2=70$ MHz,
$g_0=0.70$.

Figure 11.
Dimensionless decrements λ/f_0 for all betatron modes, and the real part of the feedback system gain $G(\omega)$ (solid line) for the parameters of Figure 10.
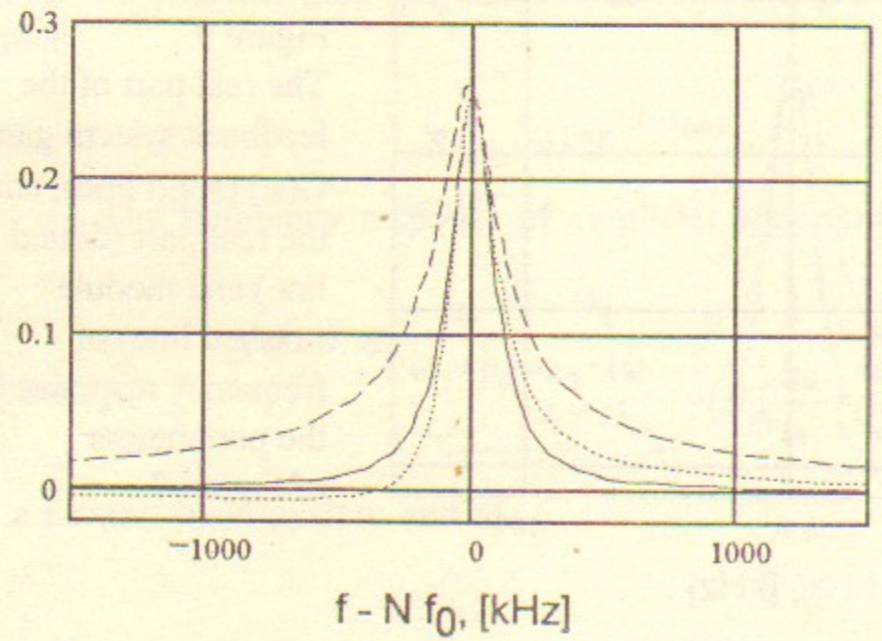

Figure 12.
The real part of the feedback system gain $G(\omega)$ (solid line), and the real part (dotted line) and module (dashed line) of frequency response for the parameters of Figure 10.
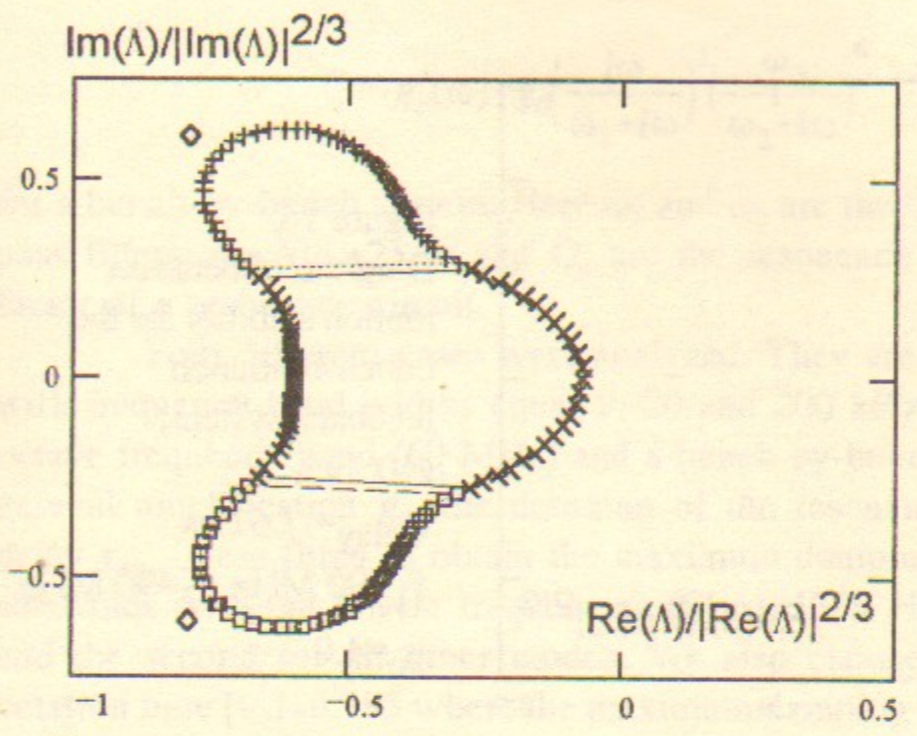

Figure 13.
Diagram of betatron motion stability;
$v=0.395$,
$Q=2$, $\tau_{delay}=-3.9$ ns
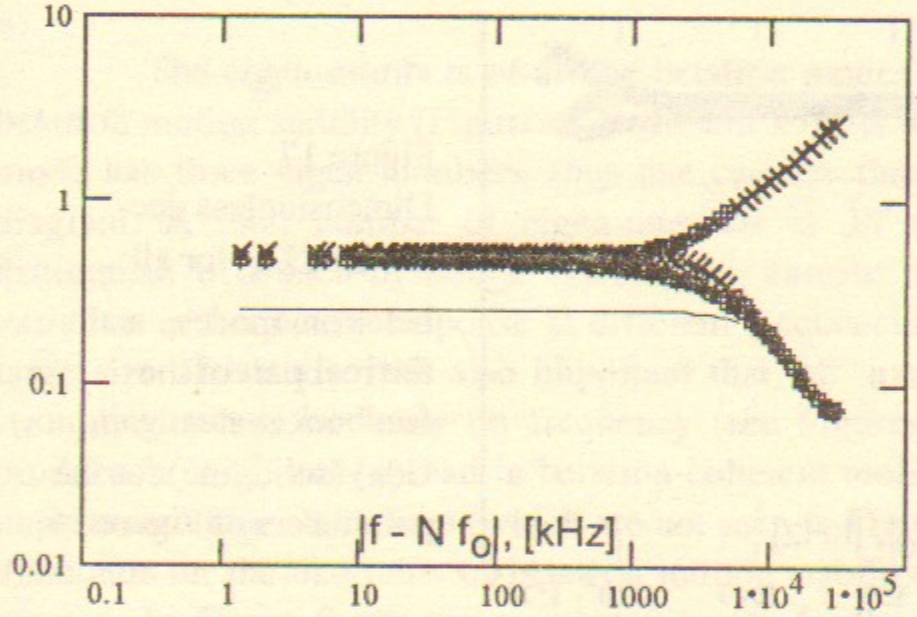$f_1=50$ MHz, $f_2=70$ MHz,
$g_0=0.66$.

Figure 14.
Dimensionless decrements λ/f_0 for all betatron modes, and the real part of the feedback system gain $G(\omega)$ (solid line) for the parameters of Figure 13.

Figure 15.
The real part of the feedback system gain $G(\omega)$ (solid line), and modules of frequency responces for the feedback system (dashed line) and the amplifier (dotted line) for the parameters of Figure 13.
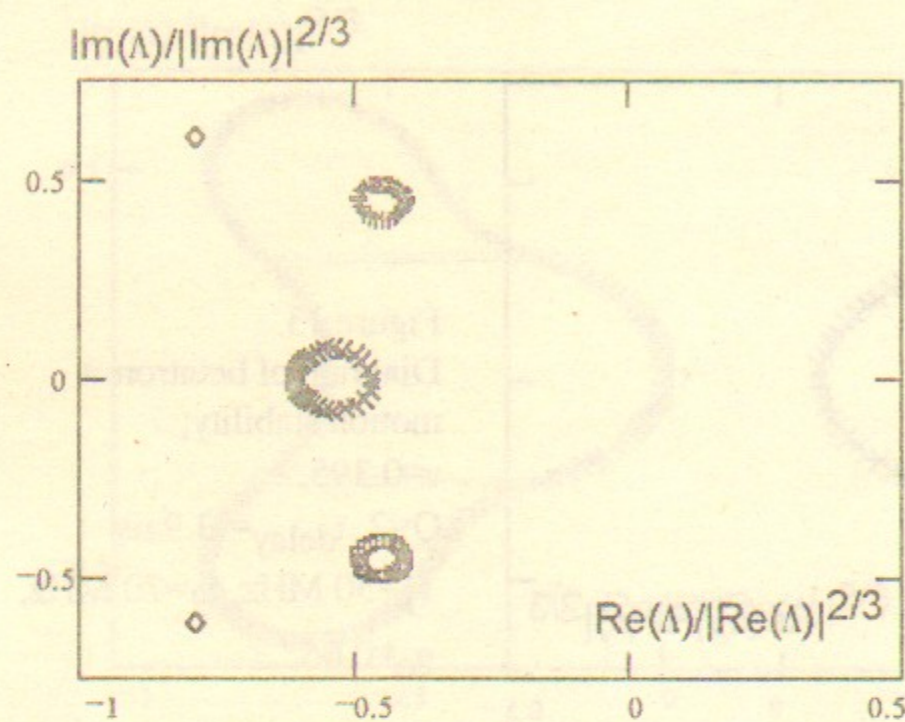
Figure 16.
Diagram of betatron motion stability for the bunch-by-bunch feedback system;
$\nu=0.395$,
$\tau_{delay}=-7.67$ ns
$f_1=90$ MHz, $f_2=90$ MHz,
$g_0=4.0$

Figure 17.
Dimensionless decrements λ/f_0 for all betatron modes, and the real part of the feedback system gain $G(\omega)$ (solid line) for the parameters of Figure 16.
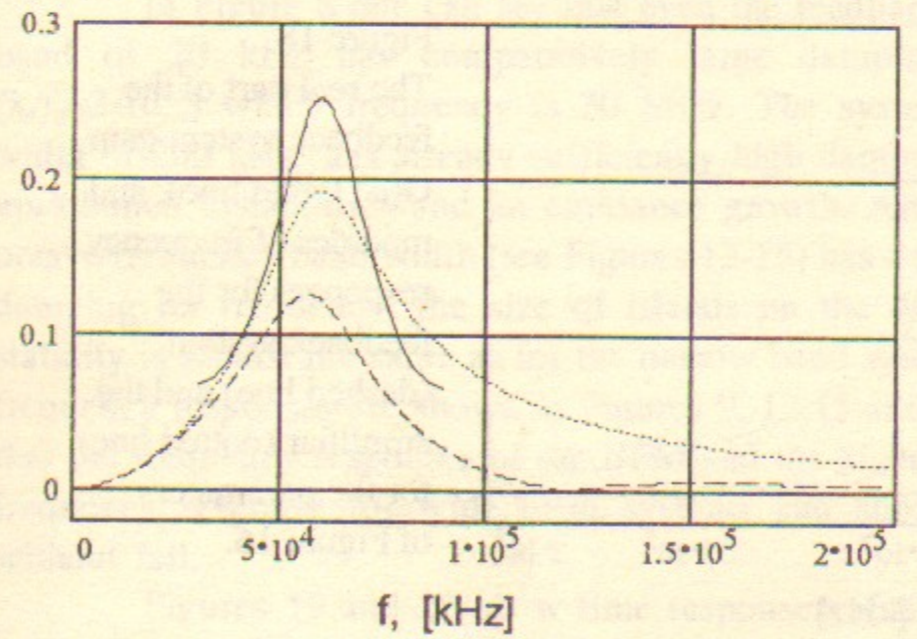

$|f - N f_0|$, [kHz]

Figure 18.
The real part of the feedback system gain $G(\omega)$ (solid line), and modules of frequency responces for the feedback system (dashed line) and the amplifier (dotted line) for the parameters of Figure 16.
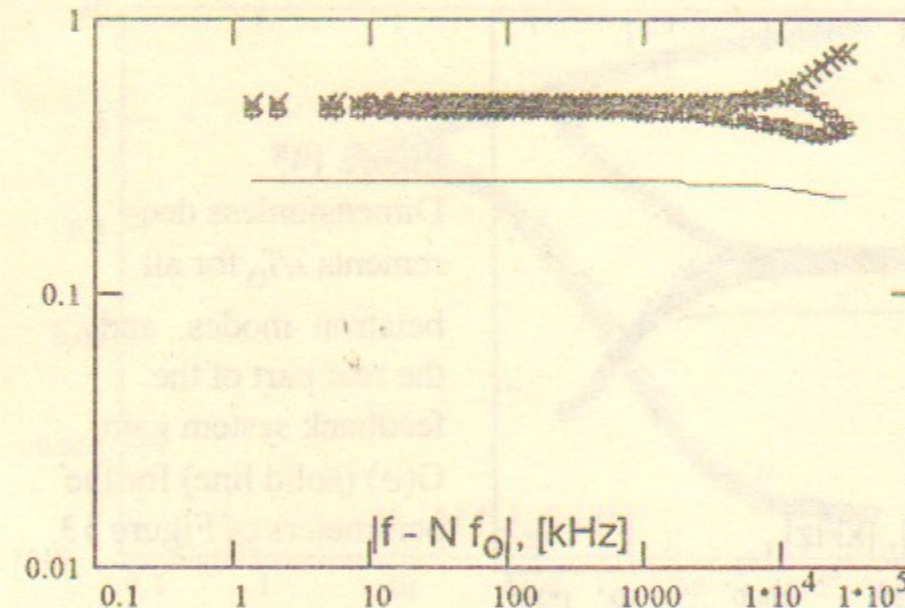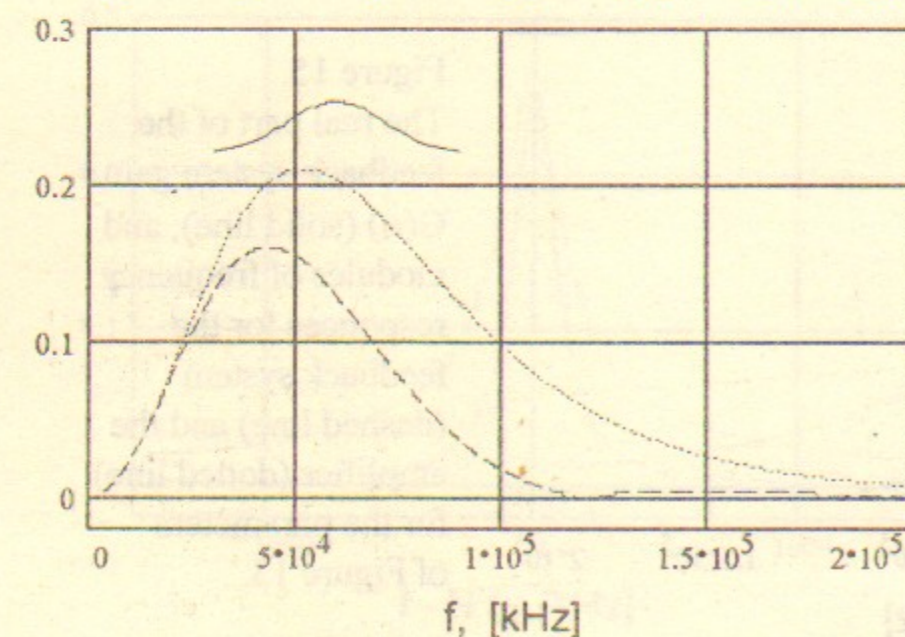
f, [kHz]

$$g_a(\omega)=g_0\left(\frac{i\omega}{\omega_1+i\omega}\right)^2\left(\frac{\omega_2}{\omega_2+i\omega}\right)^6 \tag{58}$$

for a bunch-by-bunch system. Here ω_1 and ω_2 are the frequencies of low and high pass filters, $\omega_c=N\omega_0+2\pi\cdot\delta f$ and Q_c are the resonance frequency and the quality factor of a resonance circuit.

Four different cases were analyzed. They are: two narrow band systems with frequency band widths equal to 20 and 200 kHz, a wide band system with octave frequency band (60 MHz) and a bunch-by-bunch system. For all cases the general amplification g_0, the detuning of the resonance circuit δf and the time delay τ_{delay} were fitted to obtain the maximum damping: the first for the betatron sidebands with the lowest frequencies ($f_0[\nu_0]=1359$ Hz and $f_0(1-[\nu_0])=2082$ Hz), and the second for all other modes. We also choose the fractional part of the betatron tune $[\nu_0]=0.395$ where the maximum damping can be obtained (see Figure 4).

The eigen-numbers of all the betatron modes are plotted on diagrams of betatron motion stability (Figures 7,10,13 and 16). As was shown in Section 4 each mode has three eigen-numbers, thus one can see three separate islands on each diagram. A total number of eigen-numbers is $3N$ (≈50000 for the SSC). In distinguish of bunch-by-bunch system, the narrow band systems have a large variation in frequency response at different frequencies what determines a rather large size of islands. It is also important that the narrow band system damping strongly depends not only on frequency (see Figures 8,11,14 and 17) but also produces a large tune spread in betatron coherent motion of different modes. The unperturbed eigen-numbers (which are not seen in Figures 7 and 10) are shown by diamonds on the diagrams of betatron motion stability.

In Figure 8 one can see that even the feedback system with a frequency band of 20 kHz has comparatively large damping for the highest mode ($\lambda/f_0\approx3\cdot10^{-5}$) which frequency is 30 MHz. The system with a frequency band width of 200 kHz has already sufficiently high damping decrements to damp all multibunch instabilities and an emittance growth. Although the system with an octave frequency band width (see Figures 13-15) has a rather small variation of the damping on frequency, the size of islands on the diagram of betatron motion stability is almost the same as for the narrow band systems. The feedback system frequency responses are shown in Figures 9, 12,15 and 18. It is necessary to note that the frequency responses of the BPM and the kicker strongly change the total frequency response for wide band systems and should be taken into account without fail.

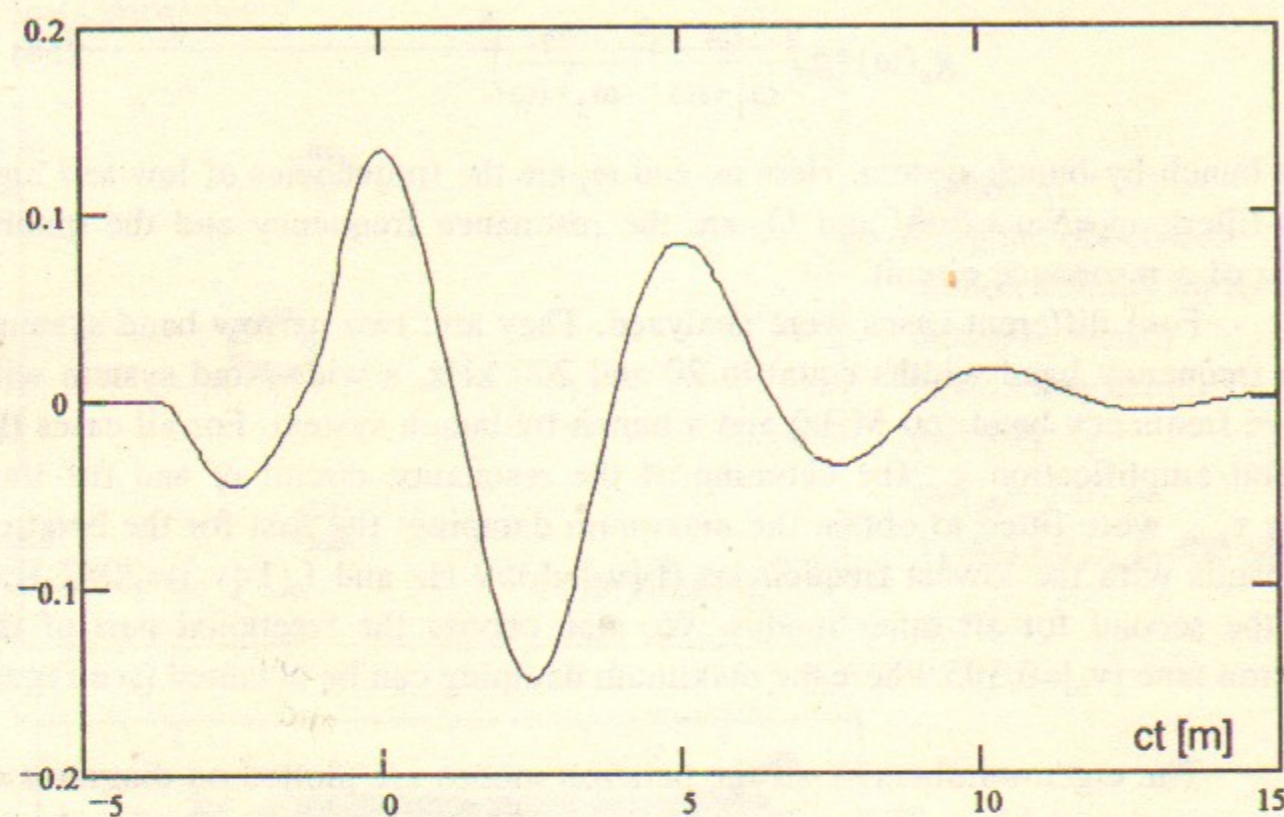Figures 19 and 20 show time responses of the feedback system for the

Figure 19. Time response of the feedback system for the parameters of Figure 13.
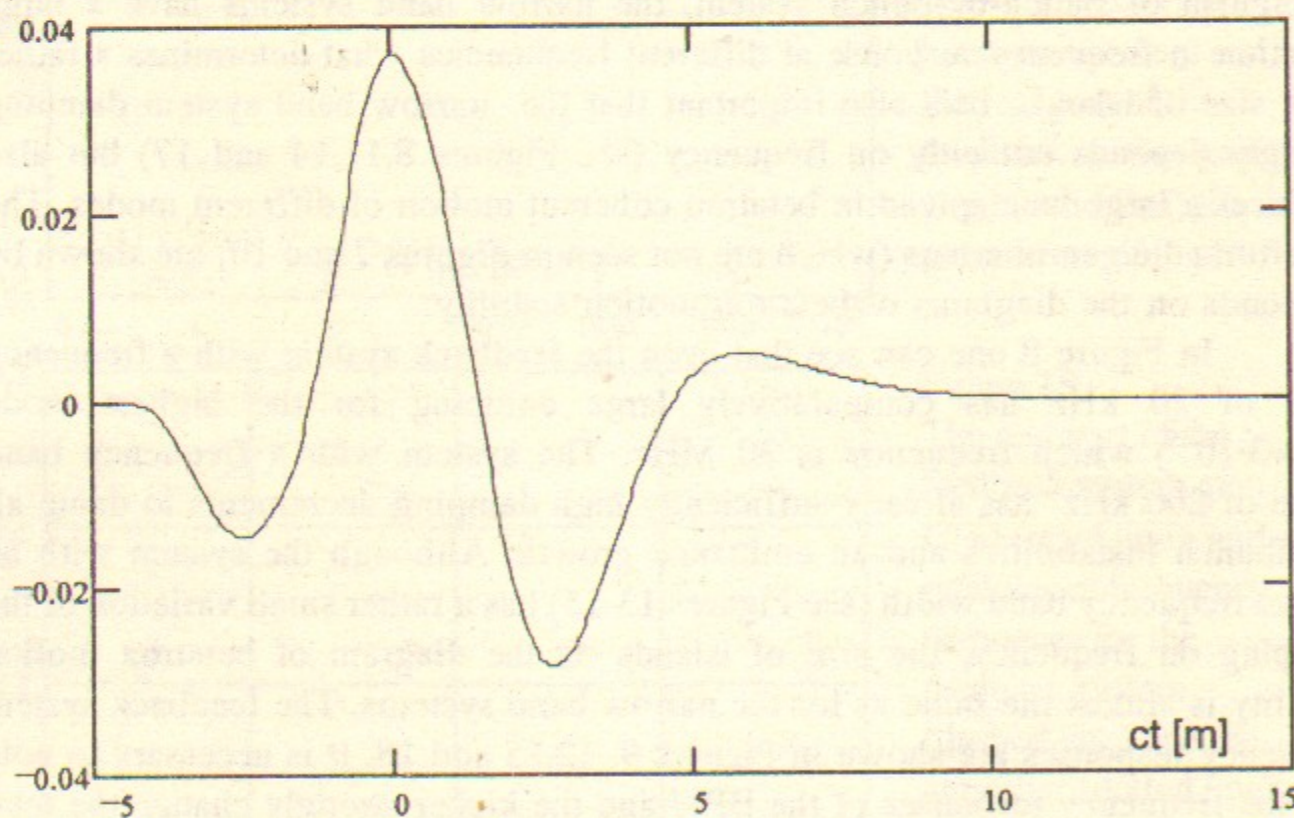

Figure 20. Time response of the bynch-by-bunch feedback system with parameters of Figure 16.

cases of the octave band width system and the bunch-by-bunch system. One can see that an octave bandwidth is not sufficient to suppress coupling between bunches.

5.3. The Emittance Growth due to Feedback System

In Section 3.2 we obtained the emittance growth rate due to feedback system noise for the case of the bunch-by-bunch system where we neglected a dependence of damping decrement on frequency and suggested a zero bunch length. Now we will obtain the emittance growth rate for the general case of the multibunch feedback system and final bunch length.

So as the noises at frequencies of different modes are independent, each of them independently contributes to the emittance growth. To take into account of them independently contributes to the emittance growth. To take into account the dependance of damping on frequency one should replace g by $2\lambda_q/f_0$ in Eqs.(9) and (10) and rewrite them as

$$\left(\frac{d\epsilon}{dt}\right)_{n1} \approx \frac{\beta_2 \omega_0^2 \xi^2}{4\pi} \sum_{q=0}^{N-1} \sum_{k=-\infty}^{\infty} \left(\frac{3.3}{4\lambda_q^2/f_0^2 + 3.3\xi^2} + 67\right) S_{noise}(\omega_{q,k}) ,\qquad(59)$$

where $\omega_{q,k}=\omega_0(\nu-q-Nk)$, $S_{noise}(\omega)$ is the noise spectral density of the kicker angle kicks and λ_q is determined by Eq.(44).

In addition to the above considered case of emittance growth, where the noise kicks affect a bunch as a whole (rigid bunches) there is another mechanism affecting the emittance growth. In this case a change of kick value along the bunch excites the bunch quadrupole motion in phase space. This motion is not affected by the feedback system, therefore the emittance growth excited by these kicks is not suppressed by the feedback system as well. Because the frequency band width is larger than the revolution frequency one can consider any two sequential kicks of the bunch as independent. Then the emittance growth rate is equal to[8]

$$\left(\frac{d\epsilon}{dt}\right)_{n2} = \frac{f_0}{2}\beta_2\langle\Delta\theta^2\rangle ,\qquad(60)$$

where

$$\langle\Delta\theta^2\rangle=\frac{1}{2\pi\tau_s}\int_{-\infty}^{\infty}\exp\left(-\frac{t^2}{2\tau_s^2}\right)\langle(\theta(t)-\bar\theta)^2\rangle dt=$$

$$=\frac{1}{2\pi\tau_s}\int_{-\infty}^{\infty}\exp\left(-\frac{t^2}{2\tau_s^2}\right)\left(\langle\theta^2(t)\rangle+\langle\bar\theta^2\rangle-2\langle\theta(t)\bar\theta\rangle\right)dt \tag{61}$$

is the r.m.s. differential kick angle, $c\tau_s$ is the longitudinal bunch length and

$$\bar\theta=\frac{1}{2\pi\tau_s}\int_{-\infty}^{\infty}\exp\left(-\frac{t^2}{2\tau_s^2}\right)\theta(t)dt \tag{62}$$

is an average beam kick for one passage and the angular brackets denote the averaging over many passages. Substituting Eq.(62) to Eq.(61), taking into account the connection between the noise correlation function and its spectral density

$$\langle(\theta(t_1)\theta(t_2))\rangle\equiv K(t_1-t_2)=\int_{-\infty}^{\infty}S_{noise}(\omega)e^{i\omega(t_1-t_2)}d\omega \tag{63}$$

and integrating over t, one has the r.m.s. differential kick

$$\langle\Delta\theta^2\rangle=\int_{-\infty}^{\infty}S_{noise}(\omega)\left(1-e^{-\omega^2\tau_s^2}\right)d\omega \quad, \tag{64}$$

and finally the emittance growth rate due to the feedback system noise

$$\left(\frac{d\epsilon}{dt}\right)_n=\left(\frac{d\epsilon}{dt}\right)_{n1}+\left(\frac{d\epsilon}{dt}\right)_{n2}\approx$$

$$\approx\frac{\beta_2\omega_0^2\xi^2}{4\pi}\sum_{q=0}^{N-1}\sum_{k=-\infty}^{\infty}\left(\frac{3.3}{4\lambda_q^2/f_0^2+3.3\xi^2}+67\right)S_{noise}(\omega_{q,k})+$$

$$+\frac{\beta_2\omega_0}{4\pi}\int_{-\infty}^{\infty}S_{noise}(\omega)\left(1-e^{-\omega^2\tau_s^2}\right)d\omega \quad, \tag{65}$$

For thorough design of the feedback system the main source of the noise is the thermonoise of preamplifiers

$$U_\omega^2=A\frac{kT\rho}{\pi} \quad, \tag{66}$$

where $A\approx1$ characterizes the excess of preamplifier noise over thermonoise of the input impedance ρ. Taking into account the feedback system amplification and kicker transfer function, we obtain the spectral density of the angle kicks of the kicker

$$S_{noise}(\omega)=\frac{4e^2L_p^2}{E^2a^2}\frac{\sin^2(\omega L/c)}{(\omega L/c)^2}|K_0(\omega)|^2\frac{AkT\rho}{\pi} \quad. \tag{67}$$

The feedback system noise is the most dangerous for the bunch-by-bunch system. Figure 21 shows the dependencies of the emittance growth time

$$\tau_\epsilon=\left(\frac{1}{\epsilon}\frac{d\epsilon}{dt}\right)^{-1} \tag{68}$$

on damping decrement of the mode with the lowest frequency for the bunch-by-bunch system and the narrow band system with a frequency band of 200 kHz. It is suggested that for both systems: $A=2$, $T=300$ K, $\rho=50$ Ω, $\beta_1=\beta_2=450$ m, $a=1.7$ cm, E=20 TeV and $\xi=0.0036$ (4 IP). The other parameters of the systems are shown in captions to Figures 16 and 10, respectively. We use here the constant A equal to 2 because of the noise from the previous turn is added to the noise of the current turn in the notch filter that doubles the noise spectral power. If for the narrow band system the contribution of the second addend in Eq.(65) is negligible in comparison with the first one, then for the wide band system the second addend is much larger than the first one. To demonstrate that, the emittance growth time for zero bunch length and the wide band system are shown in Figure 21 as well. Although the difference in the frequency band widths is very large (≈200), the difference in emittance growth times is much smaller (≈8 at large damping). This is due to different behavior of damping and noise spectral density at high frequencies in the narrow band system (compare Figures 12 and 18). For a high frequencies the damping is proportional to the real part of the feedback system gain ($\approx\Delta\omega^{-2}$), but the noise spectral density decreases much slower than the gain itself ($\approx\Delta\omega^{-1}$). Although the r.m.s. kick value is much larger for the wide band system the feedback system strongly suppresses the emittance growth rate for all harmonics so that the integral effect is only slightly higher than for the narrow band system. One can see that even in the case of the bunch-by-bunch system the noise of the feedback system can be done small enough so that the emittance growth is small yet in comparison with its damping by the synchrotron radiation
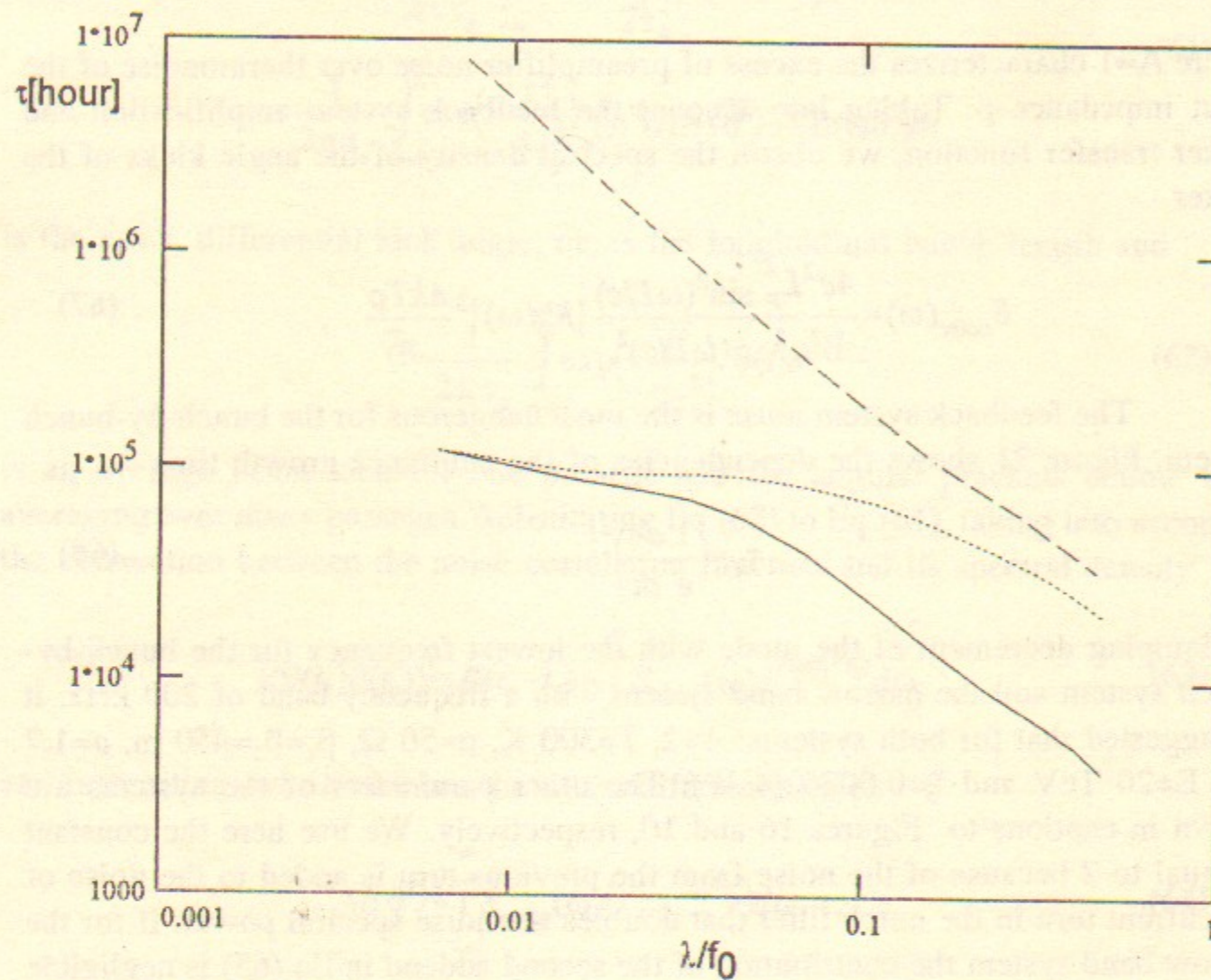
Figure 21. Dependence of the emittance growth time on damping decrement:
solid line - the wide band feedback system,
dotted line - the wide band system for zero bunch length,
dashed line - the narrow band feedback system with a frquency band of 200 kHz.

(12 hour). Although the required level of the feedback system noise is obtained much easier in the narrow band system, one can conclude that the thermonoise of the amplifiers does not impose principal limitations on the feedback system design even for the bunch-by-bunch system.

Discussion

In our numerical examples we used the fractional part of the collider tune equal to 0.395 which is close to half integer resonance. In comparison with tunes located closer to integer resonance it has some advantages:

1. Lower required amplification to get the same damping (see Eq.45) and, consequently, smaller feedback system noises.
2. The maximum possible decrements can be achieved (see Figure 4).
3. Smaller spectral density of the external noise (Its spectral density drops very quickly with frequency increase) and, consequently, smaller emittance growth due to external noises.
4. For the narrow band system, the feedback system produces the coherent tune shift of some modes to the nearest integer or half integer resonance (see Figure 10). If the unperturbed tune is close to half integer resonance, there does not exist a mode which coherent tunes are close to integer resonance. What decouples the low frequency ground motion and coherent betatron oscillations.

Table 1 shows the parameters of the above discussed feedback systems for the case where the feedback system amplification was chosen to obtain the maximum damping for the lowest harmonic.

One can see that the choice of a frequency band of about 200 kHz allows one to obtain reasonable decrements within the whole frequency range. Nevertheless, there are two unclear questions which should be studied before accepting the final choice. The first is the study of an influence of gaps between batches on damping and stability of the narrow band system, and the second is the study of beam dynamics for the modes whose coherent frequencies are close to half integer or integer resonances (compare Figures 10 and 16).

A large number of bunches and the requirements to obtain the ultimate damping and the minimum emittance growth due to feedback system noise determine high accuracy and quality of the feedback system, i.e., the BPM resolution should be better than 1 μm, the accuracy of the delay line should be about 1-2 ns (It is about $(3-6)\cdot10^{-6}$ times smaller than the revolution time). Thus, although the feedback system can be build from the general point of view, a lot

of complicated technical problems should be solved for successful feedback system operation.

Table 1

Reference to Figure		Fig.7	Fig.10	Fig.13	Fig.16
Central frequency	[MHz]	60	60	60	60
Frequency band width(FWHM)		20 kHz	200 kHz	47MHz	75MHz
Damping decrement λ/f_0 for:					
mode with lowest frequency(1.36kHz)		0.374	0.457	0.466	0.46
mode with highest frequency(30MHz)		$3 \cdot 10^{-5}$	$2.7 \cdot 10^{-4}$	0.08	0.4
Amplification, $K_0 \cdot 10^{-5}$		6.34	6.14	5.88	6.24
Emittance growth suppression for					
extern.noise at 1.36 kHz and 4 IPs		1060	1090	1090	1090
Emittance growth time	[hour]	$2.8 \cdot 10^5$	$3.4 \cdot 10^4$	6300	3800
R.M.S.kick at equilibrium	[nrad]	$7 \cdot 10^{-4}$	$2 \cdot 10^{-3}$	$2 \cdot 10^{-2}$	$3 \cdot 10^{-2}$
Noise power per kicker plate at					
equilibrium	[mW]	0.4	4	430	770
Effective BPM resolution	[μm]	0.002	0.005	0.05	0.07
Peak power for damping of 5 μm					
betatron oscillations	[kW]	~2	~2	~2	~2

From the Table one can see that after beam damping the output power determined by the feedback system noise is rather small for all considered systems. Really, the maximum power should be determined by accuracy of the notch filter subtracting and by required dynamic range of the feedback system and is almost the same for all the systems.

References

1. D.Brigs, Low Frequency Transverse Resistive Instability in the collider. Preprint SSCL-512, June 1992.
2. F.J.Sucherer,IEEE Trans.Nucl.Sci. NS-20, 825 (1973).
3. G.Lambertson, PEP-II Cavity-Damping Measurements. Mini-Workshop on Feedback Systems for Large Hadron Colliders. Erice, Italy, November 13-21, 1992.
4. Ben Cole. Private communication.
5. W.Chou, "Collider Impedances". Report on the PDRR of Collider Arc Sections. SSCL, 1992.
6. V.V.Parkhomchuk, V.D.Shiltsev. Is Transverse Feedback System Necessary for the SSC emittance preservation? Preprint SSCL, 1993.
7. V.A.Lebedev, V.V.Parkhomchuk, V.D.Shiltsev, A.N.Skrinsky. Suppression of Emittance Growth Caused by Mechanical Vibrations of Magnetic Elements in Presence of Beam-Beam Effects in the SSC. Preprint INP 91-120, Novosibirsk 1991.
8. V.A.Lebedev, V.V.Parkhomchuk, V.D.Shiltsev, G.V.Stupakov. Emittance Growth due to Noise and its Suppression with the Feedback System in Large Hadron Colliders. SSCL-Preprint-188, Dallas,TX, March 1993.
9. V.A.Lebedev. Computer Simulations of the Emittance Growth due to Noise in Large Hadron Colliders. SSCL-Preprint-191, Dallas,TX, March 1993.